
A Signed Graph Approach to Understanding and Mitigating Oversmoothing

Jiaqi Wang^{1*} Xinyi Wu^{2*} James Cheng¹ Yifei Wang^{3†}

¹ The Chinese University of Hong Kong ²MIT IDSS & LIDS ³MIT CSAIL
`{jqwang23, jcheng}@cse.cuhk.edu.hk` `{xinyiwu, yifei_w}@mit.edu`

Abstract

Deep graph neural networks (GNNs) often suffer from oversmoothing, where node representations become overly homogeneous with increasing depth. While techniques like normalization, residual connections, and edge dropout have been proposed to mitigate oversmoothing, they are typically developed independently, with limited theoretical understanding of their underlying mechanisms. In this work, we present a unified theoretical perspective based on the framework of signed graphs, showing that many existing strategies implicitly introduce negative edges that alter message-passing to resist oversmoothing. However, we show that merely adding negative edges in an unstructured manner is insufficient—the asymptotic behavior of signed propagation depends critically on the strength and organization of positive and negative edges. To address this limitation, we leverage the theory of structural balance, which promotes stable, cluster-preserving dynamics by connecting similar nodes with positive edges and dissimilar ones with negative edges. We propose Structural Balanced Propagation (SBP), a plug-and-play method that assigns signed edges based on either labels or feature similarity to explicitly enhance structural balance in the constructed signed graphs. Experiments on nine benchmarks across both homophilic and heterophilic settings demonstrate that SBP consistently improves classification accuracy and mitigates oversmoothing, even at depths of up to 300 layers. Our results provide a principled explanation for prior oversmoothing remedies and introduce a new direction for signed message-passing design in deep GNNs. Our code is available at <https://github.com/kokolerk/sbp>.

1 Introduction

Graph neural networks (GNNs) are a powerful framework for processing graph-structured data from diverse application domains [1, 2, 3, 4, 5, 6, 7]. Most GNN models follow the *message-passing* paradigm, where node representations are computed by recursively aggregating information from neighboring nodes along the edges [8, 9, 10, 11]. Despite their empirical success, deep GNNs often suffer from oversmoothing—the tendency of node features to become indistinguishable as layers increase—leading to performance degradation in deeper models [12, 13, 14, 15].

Numerous techniques have been proposed to mitigate oversmoothing in GNNs, including normalization layers [16, 17], residual connections [18, 19, 20], and random edge dropout [21, 22]. While empirically effective, these methods are typically developed independently, with limited theoretical understanding of the mechanisms that underlie their success. A common challenge is that many of them introduce architectural modifications that alter the message-passing process [23], making it difficult to precisely characterize their effects on propagation dynamics and the resulting node

*Equal contribution.

†Corresponding authors.

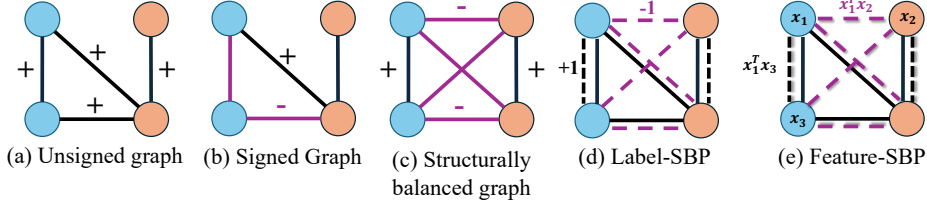


Figure 1: Examples of signed graph structures. Blue and orange circles represent nodes from different classes. Solid lines denote real edges, while dashed lines represent edges introduced by SBP. Black and purple lines indicate positive and negative edges, respectively. Let x_i be the node features for node i . (a) Initial unsigned graph. (b) Signed graph. (c) Ideal structurally balanced graph. (d),(e) Graphs induced by Label-SBP and Feature-SBP, respectively.

representations. Moreover, their ability to prevent oversmoothing is often limited, especially in deep GNNs, where they are observed to fail to preserve discriminative node features at extreme propagation depths [16, 20, 24].

In this work, we present a unified theoretical perspective on oversmoothing in GNNs, showing that many existing mitigation techniques can be interpreted as implicitly introducing negative edges into the graph used for message-passing. We formalize this insight using the framework of signed graphs [25], where edges carry either positive or negative signs (Figure 1(b)). In this view, positive edges promote alignment, while negative edges introduce repulsion, shaping the long-term dynamics of node features under signed propagation. However, we further show that simply adding negative edges in an unstructured manner is insufficient, as the asymptotic behavior of signed message-passing depends not only on the presence of negative edges but also on the strength and organization of positive and negative edges. To address this, we turn to the theory of *structural balance* [26], which characterizes graphs where positive edges connect nodes within clusters and negative edges connect nodes across clusters (Figure 1(c)). We prove that message-passing on such graphs yields stable, cluster-preserving dynamics, preventing oversmoothing while enhancing class separation.

Motivated by this theory, we propose **Structural Balance Propagation (SBP)**, a simple, plug-and-play module without introducing learnable parameters for constructing signed graphs that promote structural balance. SBP comes in two variants: (1) Label-SBP, which assigns signs based on ground-truth labels (Figure 1(d)), and (2) Feature-SBP, which estimates signs from feature similarity for label-scarce settings (Figure 1(e)). We theoretically show that Label-SBP induces structural balance under mild conditions. Empirically, we evaluate both variants on nine synthetic and real-world benchmarks across homophilic and heterophilic settings. Our results show that SBP consistently improves classification performance and mitigates oversmoothing, validating our theoretical findings. Finally, we analyze the robustness of SBP to design choices, highlighting its adaptability and reliability across diverse GNN settings.

Our main contributions are summarized as follows:

- We provide a unified theoretical perspective showing that many oversmoothing mitigation techniques such as normalization, residual connections, and edge dropout, can be interpreted as implicitly introducing negative edges into the graph. We formalize this insight through the framework of signed graphs and further show that the asymptotic behavior of signed propagation depends critically on the strength and organization of both positive and negative edges.
- We identify structural balance as an ideal condition for resisting oversmoothing, proving that it guarantees stable, class-distinct representations under signed message-passing.
- Based on this theory, we propose Structural Balanced Propagation (SBP), a simple, plug-and-play method that constructs signed graphs designed to promote structural balance, using either label information (Label-SBP) or feature similarity (Feature-SBP).
- Extensive experiments on nine benchmarks demonstrate that SBP consistently improves classification and mitigates oversmoothing across both homophilic and heterophilic graphs. Our analysis also highlights the method’s robustness and adaptability to different design choices.

2 Related Work

Theory of Oversmoothing. The notion of oversmoothing was first introduced by [12], who observed that node representations tend to converge to a common value as GNN depth increases. Subsequent work [13, 15] provided rigorous proofs showing that this convergence occurs at an exponential rate for GCNs and attention-based GNNs. [24] further showed that oversmoothing can arise even in shallow networks under specific random graph models. [23] proved that residual connections and normalization layers can mitigate oversmoothing, but they introduce their own limitations by altering the original message-passing process.

Signed Graph-Inspired Methods. Several methods have drawn inspiration from signed graph propagation to handle heterophilic graphs [27, 28, 29, 30, 31], where vanilla GNNs tend to perform worse than on homophilic graphs. [29, 30] leveraged negative edges to encode dissimilarity and introduce repulsion in message-passing. [31] made layer aggregation coefficients learnable and observed that negative edges naturally emerge in heterophilic settings. However, [32] showed that oversmoothing can still occur in signed propagation under certain random graph models, suggesting that simply adding negative edges is not sufficient to guarantee expressive representations. This highlights a broader limitation of existing approaches, which often rely on heuristic designs without a principled understanding of when and why signed message-passing is effective. In this work, we provide a theoretical characterization of how the strength and structure of negative edges influence the asymptotic behavior of node representations, and we propose Structural Balanced Propagation (SBP) to promote stable and discriminative representations on general graphs.

3 How Oversmoothing Happen in GNNs? A Signed Graph Perspective

In this section, we present a generalized message-passing framework based on signed graphs, by incorporating both attractive (positive) and repulsive (negative) interactions. We show that many oversmoothing mitigation techniques can be reinterpreted as implicitly introducing negative edges. However, we demonstrate that presence of negative edges is not sufficient—the asymptotic behavior of signed propagation depends critically on the strength of positive and negative edges.

Signed Graphs. We represent an unsigned, undirected graph with n nodes by $\mathcal{G} = (A, X)$, where $A \in \{0, 1\}^{n \times n}$ denotes the adjacency matrix and $X \in \mathbb{R}^{n \times d}$ is the node feature matrix. For node $i, j \in \{1, 2, \dots, n\}$, $A_{i,j} = 1$ if and only if node i, j are connected by an edge in \mathcal{G} and $X_i \in \mathbb{R}^d$ represents the features of node i . We let $\mathbb{1}_n$ be the all-one vector of length n and $D = \text{diag}(A\mathbb{1}_n)$ be the degree matrix of \mathcal{G} .

A signed graph associates each edge with a positive or negative sign, capturing the notion of attraction or repulsion between nodes. In this paper, we extend \mathcal{G} to the signed graph $\mathcal{G}_s = \{A^+, A^-, X\}$ where $A^+, A^- \in \{0, 1\}^{n \times n}$ are the positive and negative adjacency matrices capturing positive and negative edges, with the degree matrix $D_+ = \text{diag}(A^+\mathbb{1}_n)$ and $D_- = \text{diag}(A^-\mathbb{1}_n)$, respectively.

Signed Graph Propagation. Following [25, 33], we define the signed propagation which happen over both positive and negative edges with neighboring nodes [25] as

$$X_i^{(k)} = (1 - \alpha + \beta)X_i^{(k-1)} + \frac{\alpha}{D_i^+} \sum_{j \in N_i^+} X_j^{(k-1)} - \frac{\beta}{D_i^-} \sum_{j \in N_i^-} X_j^{(k-1)}, \quad (1)$$

where N_i^+ and N_i^- represent the set of positive and negative neighbors for node i , D_i^+ and D_i^- represent the positive and negative degrees for node i , respectively.

To allow for a general formulation, we introduce two hyperparameters: $\alpha, \beta > 0$, which control the strength of the propagation over the positive and negative edges, respectively. In particular, when $\beta = 0$ and $\alpha = 1$, (1) would correspond to the unsigned graph propagation $X_i^{(k)} = \frac{1}{D_i^+} \sum_{j \in N_i^+} X_j^{(k-1)}$ in vanilla message-passing.

Prior Methods from the Lens of Signed Graphs. Many previously proposed oversmoothing mitigation techniques can be reinterpreted as special cases of the signed graph propagation in (1). In particular, we observe the following:

Proposition 3.1 *Normalization layers, residual connections, and random edge dropout can all be expressed as instances of signed graph propagation in (1), where the vanilla unsigned message-passing*

is modified by implicitly injecting non-trivial negative edges. A summary of these correspondences is provided in Table 5 in Appendix E.

To isolate the effect of signed propagation on oversmoothing, we focus our theoretical analysis on the linear setting by removing the activation function and setting $\sigma(x) = x$, as in prior works [9, 24]. In the following theorem, we formally characterize how the strength of negative edges governs the long-term behavior of node representations.

Theorem 3.2 *Suppose that in a signed graph \mathcal{G}_s , where A^+ represents a connected graph and $X_i^{(k)}$ represents the value of node i after k propagation steps under (1). Then for any $0 < \alpha < 1/\max_{i \in X} D_i^+$, there exists a critical value $\beta_* \geq 0$ such that:*

- (i) *if $\beta < \beta_*$, then we have $\lim_{k \rightarrow \infty} X_i^{(k)} = \sum_{j=1}^n X_j^{(0)}/n$ for all initial values $X_i^{(0)}$;*
- (ii) *if $\beta > \beta_*$, then $\lim_{k \rightarrow \infty} \|X^{(k)}\| = \infty$ for almost all initial values w.r.t. Lebesgue measure.*

The proof is provided in Appendix C. Theorem 3.2 highlights the pivotal role of the negative edge weight β : it acts as a repulsive force that counterbalances the homogenizing effect of positive-edge aggregation. When β is small, especially in the extreme case where $\beta = 0$, negative edges vanish from the dynamics, and the model degenerates into standard unsigned propagation, leading to inevitable oversmoothing, regardless of the choice of α . Crucially, although increasing β can prevent oversmoothing by preserving heterogeneity in node representations, excessively strong repulsion causes the dynamics to become unstable, with representations diverging toward infinity. This tradeoff poses a challenge: how can we retain the benefits of negative edges to mitigate oversmoothing without destabilizing the model?

To address this, we turn to the theory of structural balance, which characterizes configurations of signed graphs where the tension between positive and negative edges is globally well-structured.

4 Our Proposal: Structural Balance Propagation

In this section, we propose that message-passing over *structurally balanced* signed graphs exhibit controllable and stable asymptotic behavior, making them theoretically well-suited for mitigating oversmoothing in deep GNNs. Building on this insight, we introduce Structural Balanced Propagation (SBP), a simple and effective approach that explicitly promotes structural balance in the constructed signed graph.

4.1 Asymptotic Behavior of Propagation over Structurally Balanced Graphs

In the previous section, we demonstrated that oversmoothing arises when the influence of negative edges is insufficient to counteract the homogenizing effect of positive-edge propagation. Conversely, overly strong negative edges lead to divergence and instability. This reveals a fundamental tension in signed message-passing: to avoid oversmoothing while ensuring stability, the distribution and strength of signed edges must be carefully controlled.

To address this challenge, we turn to a special class of signed graphs known as structurally balanced graphs. These graphs encode an ideal configuration in which positive edges connect nodes within the same cluster, and negative edges span across clusters. Crucially, under signed propagation, such structure leads to stable asymptotic behavior that preserves intra-cluster similarity and inter-cluster distinction—precisely the property needed to resist oversmoothing and enhance classification performance in deep GNNs [24]. Formally, following [25, 26], we define structural balance as follows:

Definition 4.1 (Structurally Balanced Graph) *A signed graph \mathcal{G}_s is called **structurally balanced** if there is a partition of the node set into $V = V_1 \cup V_2$ with V_1 and V_2 being nonempty and mutually disjoint, where any edge between the two node subsets V_1 and V_2 is negative, and any edge within each V_i is positive.*

The structural balance property partitions the graph into two disjoint node sets, V_1 and V_2 , such that positive edges connect nodes within the same group, while negative edges connect nodes

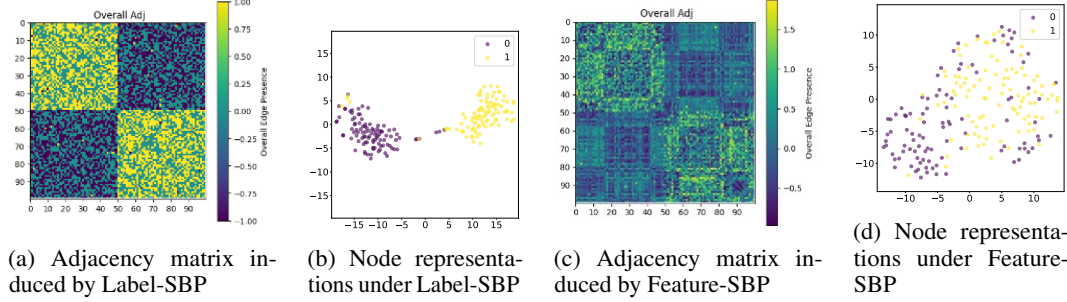


Figure 2: The visualization of the signed adjacency matrix $A^+ - A^-$ induced by SBP and resulting node representations on 2-CSBM under Layer= 300. (a)(c): The X-axis and Y-axis denote the nodes 0-99, where 0-49 is from class 0 and 50-99 is from class 1. (b)(d): The t-SNE visualization of the node representations learned by SBP.

across groups, as illustrated in Figure 1 (c). This organization of edge signs induces well-structured propagation dynamics. We characterize the asymptotic behavior of signed message-passing on structurally balanced graphs as follows:

Theorem 4.2 *Assume that node i is connected to node j and $X_i^{(k)}$ represents the value of node i after k propagation steps in (1). $\mathcal{F}(z)_c$ is a bounded function such that: if $z < -c$, $\mathcal{F}(z)_c = -c$; if $z > c$, $\mathcal{F}(z)_c = c$; if $-c < z < c$, $\mathcal{F}(z)_c = z$. Let $\theta = \alpha$ if the edge $\{i, j\}$ is positive and $\theta = -\beta$ if the edge $\{i, j\}$ is negative. Consider the constrained signed propagation update:*

$$X_i^{(k+1)} = \mathcal{F}_c((1 - \theta)X_i^{(k)} + \theta X_j^{(k)}). \quad (2)$$

Let $\alpha \in (0, 1/2)$. Assume that \mathcal{G}_s is a structurally balanced complete graph under the partition $V = V_1 \cup V_2$. When β is sufficiently large, we have that

$$\mathbb{P} \left(\lim_{k \rightarrow \infty} X_i^{(k)} = c, i \in V_1; \lim_{k \rightarrow \infty} X_i^{(k)} = -c, i \in V_2 \right) = 1. \quad (3)$$

The proof is provided in Appendix D. The result above shows that if the graph is structurally balanced and the signed graph propagation is constrained with a bounded function \mathcal{F}_c , node features converge asymptotically to group-specific values under the propagation rule defined in (1). Moreover, nodes belonging to different groups are repelled from one another, resulting in asymptotically distinct representations across groups. This behavior implies that structurally balanced graphs provide a provable mechanism for mitigating oversmoothing, by assigning positive and negative edge signs in accordance with the underlying class structure—encouraging intra-class consistency while maintaining inter-class separation.

Remark 4.3 *The two-group result above can be generalized to multiple groups by introducing a more general notion known as weak structural balance. See detailed discussion in Appendix G.*

4.2 Method: Design Structural Balance Propagation for GNNs

Building on the theoretical insights from the previous section, we propose **Structural Balance Propagation (SBP)**, a principled approach for promoting structural balance in the message-passing process of GNNs. Specifically, we introduce two variants: Label-SBP and Feature-SBP, which inject signed edges that approximate structurally balanced configurations using label supervision and feature similarity, respectively.

Label Induced Structural Balance Propagation (Label-SBP). We extend the original adjacency matrix to the positive and negative ones. Let the positive adjacency matrix be the original adjacency matrix $A^+ = A$, we then construct a label-informed negative adjacency matrix A_l^- , designed to introduce repulsion between classes and promote attraction within classes. Specifically, for node pairs with known labels, we assign a value of 1 if the labels differ (to repel), -1 if the labels match (to attract), and 0 otherwise to preserve the original structure when labels are unknown. Formally:

$$(A_l^-)_{ij} = \begin{cases} 1 & \text{if } y_i \neq y_j, \\ -1 & \text{if } y_i = y_j, \\ 0 & \text{otherwise,} \end{cases} \quad (4)$$

where y_i is the ground truth label for node i . We theoretically show that Label-SBP induces a structurally balanced graph under mild conditions (see formal statement and proof in Appendix H).

Theorem 4.4 (Informal) *Assume class labels are balanced, and let p denote the ratio of labeled nodes. As p increases, the degree of structural balance improves, and the graph becomes fully structurally balanced when $p = 1$.*

Figure 2a shows the signed adjacency matrix $A^+ - A_l^-$, constructed by Label-SBP on the Contextual Stochastic Block Model with two blocks (2-CSBM) [34], highlighting its structural balance: positive edges appear within label blocks, and negative edges span between them. Figure 2b visualizes the learned node representations, demonstrating that Label-SBP achieves clear class separation even at depth $L = 300$, attaining a high classification accuracy of 97.50%, which is consistent with Theorem 4.2.

Furthermore, to tackle scenarios where labels are scarce, we propose a variant of SBP that estimates the negative adjacency matrix based on feature similarities.

Feature Induced Structural Balance Propagation (Feature-SBP). We retain the positive adjacency matrix in Feature-SBP as in Label-SBP, setting $A^+ = A$. To construct the negative adjacency matrix A_f^- , We leverage feature similarity to assign positive and negative edges—promoting attraction between similar nodes and introducing repulsion between dissimilar ones—without relying on labels. Specifically, we define:

$$A_f^- = -X^{(0)} X^{(0)\top}, \quad (5)$$

where $X^{(0)}$ denotes the initial node features. While this approach may be less precise than Label-SBP due to the absence of label supervision, it leverages the full feature set, including test nodes, to improve the overall alignment with structural balance across the graph.

Figure 2c and 2d illustrate the signed adjacency matrix $A^+ - A_f^-$ and learned node representations on the 2-CSBM data. Notably, Feature-SBP preserves structural balance patterns similar to Label-SBP and achieves strong classification performance with an accuracy of 80.00%.

Implementation Details. We implement the constrained function \mathcal{F}_c in Theorem 4.2 by Layer-Norm [35]. To avoid numerical instability for repeated message-passing, we ensure that the sum of the coefficients combining the node representations $X^{(k)}$ and the node representations updates by our SBP remains 1. We employ a row-stochastic adjacency matrix \hat{A} as the positive adjacency matrix, denoted \hat{A}^+ . Additionally, we apply the softmax function to the negative matrix, resulting in $\hat{A}^- = \text{softmax}(A^-)$. As a result, Label/Feature-SBP can be written as:

$$X^{(k+1)} = (1 - \lambda)X^{(k)} + \lambda \left(\alpha \hat{A}^+ X^{(k)} - \beta \hat{A}^- X^{(k)} \right).$$

where $0 < \lambda < 1$, $\alpha, \beta > 0$ are the hyperparameters controlling the strength of positive and negative edges.

Scalability on Large-Scale Graphs. Although SBP improves the structural balance property for message-passing in GNNs, it may reduce graph sparsity and cause out-of-memory issues on large-scale graphs. To adapt SBP in large-scale graphs, we propose Label-SBP-v2, which removes only inter-class edges instead of explicitly adding negative ones. This preserves sparsity by avoiding the addition of new edges, thereby reducing computational overhead while still encouraging structural balance.

For Feature-SBP, the original negative adjacency matrix has quadratic complexity $\mathcal{O}(n^2d)$, which is prohibitive for large n . To improve efficiency, we replace the node-level similarity matrix $-XX^\top \in \mathbb{R}^{n \times n}$ with its transposed form $-X^\top X \in \mathbb{R}^{d \times d}$, following [16]. This shifts repulsion to the feature dimension and reduces complexity to $\mathcal{O}(nd^2)$, which is significantly more scalable when $n \gg d$. More detailed analysis is provided in Appendix I.3.

5 Experiments

In this section, we conduct a comprehensive evaluation of SBP on various benchmark datasets, including both homophilic and heterophilic graphs. We aim to answer the following three key research questions:

Table 2: Node classification accuracy using standard-depth GNNs (%). Best results are highlighted in blue; second-best results are shown in gray. Overall, SBP performs best on both homophilic and heterophilic datasets.

$H(G)$ Dataset	0.81 Cora	0.74 Citeseer	0.80 PubMed	0.22 Squirrel	0.38 Amazon-ratings	0.21 Texas	0.11 Wisconsin	0.30 Cornell
MLP	48.82 \pm 0.98	47.89 \pm 1.21	69.20 \pm 0.83	32.58 \pm 0.19	38.14 \pm 0.03	73.51 \pm 2.36	70.98 \pm 1.18	68.11 \pm 2.65
SGC	80.21 \pm 0.07	71.88 \pm 0.27	76.99 \pm 0.38	43.30 \pm 0.30	42.83 \pm 0.04	45.95 \pm 0.00	47.06 \pm 0.00	48.11 \pm 3.15
BatchNorm	77.90 \pm 0.00	60.85 \pm 0.09	77.15 \pm 0.09	44.22 \pm 0.11	39.68 \pm 0.01	39.73 \pm 1.24	52.94 \pm 0.00	46.49 \pm 1.08
PairNorm	80.30 \pm 0.05	70.83 \pm 0.06	77.69 \pm 0.26	46.21 \pm 0.09	42.30 \pm 0.05	51.35 \pm 0.00	58.82 \pm 0.00	51.35 \pm 0.00
ContraNorm	81.60 \pm 0.00	72.25 \pm 0.08	79.30 \pm 0.10	48.63 \pm 0.16	42.98 \pm 0.04	48.38 \pm 4.43	49.61 \pm 1.53	48.63 \pm 0.16
DropEdge	73.58 \pm 2.76	65.63 \pm 1.76	74.64 \pm 1.37	42.30 \pm 0.62	42.30 \pm 0.09	59.46 \pm 8.11	52.55 \pm 4.45	45.95 \pm 7.05
Residual	77.81 \pm 0.03	71.61 \pm 0.17	77.40 \pm 0.06	43.63 \pm 0.34	42.69 \pm 0.03	65.95 \pm 1.32	63.73 \pm 0.98	61.89 \pm 3.91
APPNP	77.78 \pm 0.93	67.42 \pm 1.31	74.52 \pm 0.49	42.15 \pm 0.17	42.47 \pm 0.03	68.38 \pm 4.37	65.10 \pm 1.71	64.59 \pm 3.30
JKNET	78.20 \pm 0.20	66.80 \pm 0.33	75.62 \pm 0.37	48.16 \pm 0.25	42.21 \pm 0.05	60.00 \pm 2.36	42.55 \pm 2.92	39.73 \pm 2.72
DAGNN	65.98 \pm 1.49	60.04 \pm 1.98	72.39 \pm 0.90	33.39 \pm 0.19	40.61 \pm 0.03	61.35 \pm 1.73	57.45 \pm 1.97	44.87 \pm 3.24
Feature-SBP	82.46 \pm 0.07	70.63 \pm 0.52	77.41 \pm 0.21	49.16 \pm 0.19	42.31 \pm 0.03	78.38 \pm 0.00	80.39 \pm 0.00	72.97 \pm 0.00
Label-SBP	82.90 \pm 0.00	73.04 \pm 0.10	80.32 \pm 0.04	45.60 \pm 0.11	42.41 \pm 0.02	78.38 \pm 0.00	80.39 \pm 0.00	70.27 \pm 0.00

- **RQ1** How does SBP perform in node classification tasks using standard-depth GNNs?
- **RQ2** How effectively does SBP mitigate oversmoothing in deep layers?
- **RQ3** How sensitive, robust, and scalable is SBP to different hyperparameters, model backbones, and graph homophily levels?

Datasets. We use nine widely-used node classification benchmark datasets (Table 7), where four of them are heterophilic (Texas, Wisconsin, Cornell, Squirrel, and Amazon-rating [36]), and the remaining four are homophilic (Cora [37], Citeseer [38], and PubMed [39]), including one large-scale dataset (ogbn-arxiv [40]). Details of these datasets, including their homophily levels, are summarized in Table 1. We also experiment on the Contextual Stochastic Block Model (CSBM) [34] to show the performance of SBP on different homophily levels with detailed settings in Appendix I.1.

Baselines and Experiment Settings. We implement SBP along with the following 10 baselines, all using the Simplified Graph Convolution Network (SGC) as the backbone GNN to ensure a fair comparison. 1) **Classic models:** MLP, vanilla SGC [9]. 2) **Normalization methods:** BatchNorm [41], PairNorm [17] and ContraNorm [16]. 3) **Edge dropping methods:** DropEdge [22]. 4) **Residual connections:** Residual, APPNP [42], JKNET [18] and DAGNN [19].

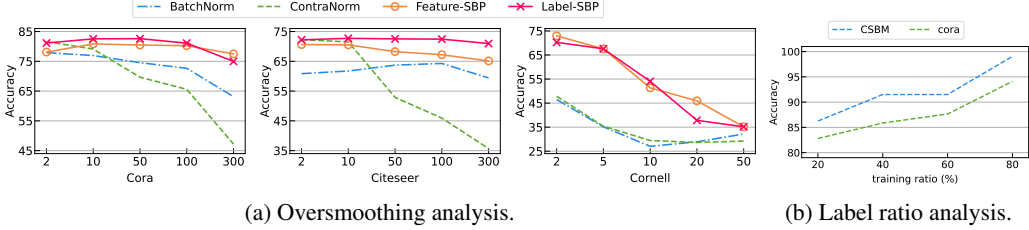
All methods are trained using the same setting, following [43]. For SBP, we select the optimal value of λ from the set $\{0.1, 0.5, 0.9\}$, fix $\alpha = 1$, and then choose the best value for β from $\{0.1, 0.5, 0.9\}$. Ablation studies on the influence of hyperparameters and the effectiveness of SBP with other GNN backbones can be found in Section 5.3.

5.1 RQ1: Node Classification Performance Using Standard-Depth GNNs

To evaluate the effectiveness of SBP under typical GNN settings, we assess its performance on node classification tasks using standard-depth models. Table 2 reports the mean node classification accuracy and standard deviation across 10 random seeds, using a 2-layer SGC backbone [44]. The results show that SBP improves node classification performance in standard-depth GNNs, yielding an average gain of 3 percentage points on homophilic graphs and 5 points on heterophilic graphs. Overall, SBP achieves superior performance across 8 datasets, with Label/Feature-SBP attaining the highest accuracy on 7 datasets.

Table 1: Summary of datasets. $H(G)$ denotes the edge homophily level, with higher values indicating more homophilic graphs.

Dataset	$H(G)$	Classes	Nodes	Edges
Cora	0.81	7	2,708	5,429
Citeseer	0.74	6	3,327	4,732
PubMed	0.80	3	19,717	44,338
Texas	0.21	5	183	295
Cornell	0.30	5	183	280
Amazon-ratings	0.38	5	24,492	93,050
Wisconsin	0.11	5	251	466
Squirrel	0.22	4	198,493	2,089
ogbn-arxiv	0.65	40	16,9343	1,166,243



(a) Oversmoothing analysis.

(b) Label ratio analysis.

Figure 3: (a) Model performance under varying the number of layers. SBP remains effective up to 300 layers, while normalization methods degrade with depth due to oversmoothing. The X-axis denotes number of layers and the Y-axis denotes accuracy. (b) Sensitivity of Label-SBP to training label ratio. Label-SBP’s performance improves with increasing label ratio, aligning with our theory. The X-axis denotes training label ratio and the Y-axis denotes accuracy.

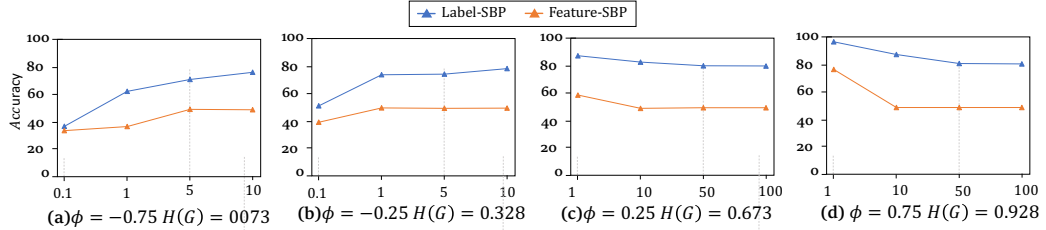


Figure 4: Impact of negative edge strength β in SBP under different homophily levels on CSBM. ϕ controls the homophily level $H(G)$. The X-axis denotes β and the Y-axis denotes accuracy. Homophilic graphs favor smaller β , while heterophilic graphs benefit from larger β values.

5.2 RQ2: Anti-Oversmoothing Analysis

We further evaluate SBP’s ability to counter oversmoothing in deep GNNs by varying the number of layers K . Figure 3(a) compares Label-/Feature-SBP against BatchNorm and PairNorm on both homophilic (Cora, Citeseer) and heterophilic (Cornell) benchmarks. For homophilic graphs, we test $K \in \{2, 10, 50, 100, 300\}$, and for the heterophilic graph, $K \in \{2, 5, 10, 20, 50\}$.

Notably, SBP maintains strong performance even at 300 layers, effectively mitigating oversmoothing in deep GNNs. In contrast, normalization-based methods exhibit substantial performance degradation as depth increases, reaffirming their vulnerability to oversmoothing [23]. Interestingly, we also observe that to maintain performance on heterophilic datasets, SBP requires a larger repulsion strength β than typical settings (e.g., $\beta \in \{0.1, 0.5, 0.9\}$). As shown in Table 12, setting $\beta > 1$ enables SBP to sustain approximately 60% accuracy in deep-layer regimes on the Cornell dataset.

5.3 RQ3: Robustness, Sensitivity, and Scalability of SBP

Sensitivity of Label-SBP to Training Label Ratio. Since Label-SBP relies on ground-truth labels to construct the negative graph, we conduct an ablation study to examine its sensitivity to the proportion of labeled training data. As shown in Figure 3(b), Label-SBP’s performance on the CSBM and Cora datasets improves with increasing label ratio when using a 2-layer SGC backbone. This aligns with our theoretical result that greater label availability leads to better structural balance in the signed graph, enhancing classification performance.

Nonetheless, even with a modest training ratio of 20%, Label-SBP achieves over 80% accuracy, while models trained with 80% labels approach 100% accuracy. Furthermore, as shown in Table 2, Label-SBP outperforms existing methods even under the default training splits of standard benchmarks, highlighting its robustness and practical effectiveness in real-world graph settings.

Analysis of Negative Edge Strength β Under Different Homophilic and Heterophilic Levels. In order to evaluate the performance of SBP on graphs with arbitrary levels of homophily, we conduct an ablation study in the CSBM setting with controllable homophilic and heterophilic levels, following the setup from [31]. We examine a wide range of β values, while keeping $\lambda = 0.5$, $\alpha = 1$ and using a hyperparameter in CSBM, ϕ , to control the homophily level. The graph homophily is measured by $H(G)$.

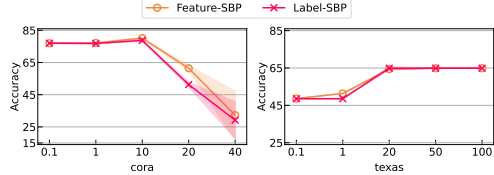


Figure 5: Impact of negative edge strength β in SBP on real graphs. The X-axis denotes β and the Y-axis denotes accuracy.

Table 3: Node classification accuracy (%) on the large-scale dataset *ogbn-arxiv*. Best results are highlighted in blue.

Model	#L=2	#L=4	#L=8	#L=16
GCN	67.32 ± 0.28	67.79 ± 0.25	65.54 ± 0.31	59.13 ± 0.95
BatchNorm	70.14 ± 0.28	70.93 ± 0.15	70.14 ± 0.43	63.24 ± 1.40
PairNorm	70.48 ± 0.20	71.59 ± 0.17	71.24 ± 0.07	68.92 ± 0.43
ContraNorm	OOM	OOM	OOM	OOM
DropEdge	64.07 ± 0.32	63.92 ± 0.27	60.74 ± 0.45	52.52 ± 0.34
Residual	66.90 ± 0.14	66.67 ± 0.25	61.76 ± 0.62	53.25 ± 0.75
Label-SBP-v2	70.55 ± 0.22	71.54 ± 0.18	71.07 ± 0.28	69.33 ± 0.59

Table 4: Performance of SBP with different GNN backbones. Best results are highlighted in blue.

	#L=2	#L=4	#L=8	#L=16	
Cora	GCN	80.68 ± 0.09	79.69 ± 0.00	74.32 ± 0.00	30.95 ± 0.00
	+Feature-SBP	80.44 ± 0.83	79.26 ± 1.18	78.56 ± 0.59	77.22 ± 0.55
	+Label-SBP	80.31 ± 0.70	79.16 ± 1.30	79.50 ± 0.00	77.43 ± 1.49
	GCNII	78.58 ± 0.00	77.76 ± 0.24	73.47 ± 3.82	78.12 ± 1.32
	+Label-SBP	78.74 ± 1.54	78.87 ± 0.00	79.14 ± 0.35	79.17 ± 0.41
	+Feature-SBP	77.95 ± 0.91	78.82 ± 0.00	78.11 ± 1.62	78.82 ± 0.29
Citesser	GCN	67.45 ± 0.54	65.62 ± 0.25	37.22 ± 2.46	22.03 ± 4.76
	+Feature-SBP	67.38 ± 0.66	66.94 ± 0.00	66.29 ± 0.02	65.35 ± 1.99
	+Label-SBP	67.23 ± 0.64	66.72 ± 0.00	66.29 ± 0.89	65.50 ± 2.13
	GCNII	61.66 ± 0.67	63.23 ± 2.31	64.58 ± 2.66	66.21 ± 0.64
	+Label-SBP	65.31 ± 0.63	63.93 ± 3.66	68.33 ± 0.99	66.46 ± 0.00
	+Feature-SBP	65.63 ± 0.87	64.43 ± 3.55	68.44 ± 1.19	66.94 ± 0.00

Figure 4 shows the performance of Feature/Label-SBP across different β values. In Figures 4(a) and (b), where $\phi < 0$ indicates heterophilic graphs, increasing β significantly improves performance. Conversely, in Figures 4(c) and (d), where $\phi > 0$ corresponds to homophilic graphs, performance deteriorates as β increases. We observe similar trends on real-world homophilic and heterophilic graph datasets, as shown in Figure 5. These results further highlight the role of β as a repulsive force in the message-passing process, supporting our signed graph perspective for understanding and mitigating oversmoothing.

Performance on Large-Scale Dataset. To preserve graph sparsity and reduce computational overhead, we adopt SBP variants designed for large-scale graphs, as detailed in Section 4. Results on the ogbn-arxiv dataset are shown in Table 3. Overall, Label-SBP-v2 matches or outperforms existing normalization methods, particularly in the deep setting $L = 16$. These results demonstrate the empirical robustness and scalability of SBP-v2, which effectively leverages label information to mitigate oversmoothing even at large scale.

SBP with Different GNN Backbones. Beyond the SGC backbone, SBP can be seamlessly integrated into other GNN architectures, consistently yielding performance gains. Table 4 shows the results for SBP applied to GCN and GCNII across various model depths. SBP improves GCN performance by up to 47 points, particularly at depth $L = 16$, and also boosts the performance of GCNII, a state-of-the-art model explicitly designed to address oversmoothing. These results further support our insight that promoting structural balance is an effective strategy for mitigating oversmoothing in deep GNNs.

Time Efficiency of SBP. SBP is highly efficient, adding only minimal overhead compared to vanilla backbones. Figure 6 reports the actual runtime of various methods integrated with SGC on CSBM. Feature-SBP is the fastest among all methods, while Label-SBP ranks third—slightly slower than DAGNN but still more efficient than the normalization-based approaches. Additional analysis of SBP’s runtime on large-scale graphs is provided in Appendix I.4.6.

6 Conclusion

In this work, we present a unified signed graph perspective on oversmoothing in GNNs, identifying structural balance as an ideal condition for preserving expressive node representations. Building on this insight, we propose Structural Balanced Propagation (SBP), a simple and plug-and-play method that constructs signed graphs to promote structural balance and mitigate oversmoothing. Extensive experiments demonstrate SBP’s robustness, scalability, and consistent performance gains

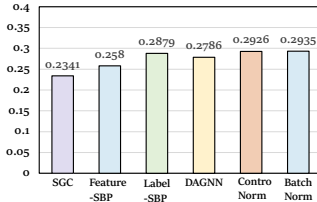


Figure 6: Real runtime (in seconds) of various methods.

across diverse settings. Beyond practical improvements, our work provides a theoretical foundation for understanding message-passing dynamics beyond vanilla GNNs and opens new directions for principled signed message-passing design.

References

- [1] M. Gori, G. Monfardini, and F. Scarselli. A new model for learning in graph domains. In *IJCNN*, 2005.
- [2] Franco Scarselli, Marco Gori, Ah Chung Tsoi, Markus Hagenbuchner, and Gabriele Monfardini. The graph neural network model. *IEEE Transactions on Neural Networks*, 2009.
- [3] Joan Bruna, Wojciech Zaremba, Arthur D. Szlam, and Yann LeCun. Spectral networks and locally connected networks on graphs. In *ICLR*, 2014.
- [4] David Kristjanson Duvenaud, Dougal Maclaurin, Jorge Aguilera-Iparraguirre, Rafael Gómez-Bombarelli, Timothy D. Hirzel, Alán Aspuru-Guzik, and Ryan P. Adams. Convolutional networks on graphs for learning molecular fingerprints. In *NeurIPS*, 2015.
- [5] Michaël Defferrard, Xavier Bresson, and Pierre Vandergheynst. Convolutional neural networks on graphs with fast localized spectral filtering. In *NeurIPS*, 2016.
- [6] Peter Battaglia, Razvan Pascanu, Matthew Lai, Danilo Jimenez Rezende, and koray kavukcuoglu. Interaction networks for learning about objects, relations and physics. In *NeurIPS*, 2016.
- [7] Yujia Li, Daniel Tarlow, Marc Brockschmidt, and Richard S. Zemel. Gated graph sequence neural networks. In *ICLR*, 2016.
- [8] Thomas N. Kipf and Max Welling. Semi-supervised classification with graph convolutional networks. In *ICLR*, 2017.
- [9] Felix Wu, Amauri Souza, Tianyi Zhang, Christopher Fifty, Tao Yu, and Kilian Weinberger. Simplifying graph convolutional networks. In *ICML*, 2019.
- [10] Petar Veličković, Guillem Cucurull, Arantxa Casanova, Adriana Romero, Pietro Liò, and Yoshua Bengio. Graph attention networks. In *ICLR*, 2018.
- [11] Keyulu Xu, Weihua Hu, Jure Leskovec, and Stefanie Jegelka. How powerful are graph neural networks? In *ICLR*, 2019.
- [12] Qimai Li, Zhichao Han, and Xiao-Ming Wu. Deeper insights into graph convolutional networks for semi-supervised learning. In *AAAI*, 2018.
- [13] Kenta Oono and Taiji Suzuki. Graph neural networks exponentially lose expressive power for node classification. In *ICLR*, 2020.
- [14] Chen Cai and Yusu Wang. A note on over-smoothing for graph neural networks. In *ICML Graph Representation Learning and Beyond (GRL+) Workshop*, 2020.
- [15] Xinyi Wu, Amir Ajourlou, Zihui Wu, and Ali Jadbabaie. Demystifying oversmoothing in attention-based graph neural networks. In *NeurIPS*, 2023.
- [16] Xiaojun Guo, Yifei Wang, Tianqi Du, and Yisen Wang. ContraNorm: A contrastive learning perspective on oversmoothing and beyond. In *ICLR*, 2023.
- [17] Lingxiao Zhao and Leman Akoglu. PairNorm: Tackling oversmoothing in gnns. *ArXiv*, 2019.
- [18] Keyulu Xu, Chengtao Li, Yonglong Tian, Tomohiro Sonobe, Ken-ichi Kawarabayashi, and Stefanie Jegelka. Representation learning on graphs with jumping knowledge networks. In *ICLR*, 2018.
- [19] Meng Liu, Hongyang Gao, and Shuiwang Ji. Towards deeper graph neural networks. In *Proceedings of the 26th ACM SIGKDD international conference on knowledge discovery & data mining*, 2020.

[20] Ming Chen, Zhewei Wei, Zengfeng Huang, Bolin Ding, and Yaliang Li. Simple and deep graph convolutional networks. In *International Conference on Machine Learning*, 2020.

[21] Taoran Fang, Zhiqing Xiao, Chunping Wang, Jiarong Xu, Xuan Yang, and Yang Yang. Dropmessage: Unifying random dropping for graph neural networks. In *AAAI Conference on Artificial Intelligence*, 2022.

[22] Yu Rong, Wenbing Huang, Tingyang Xu, and Junzhou Huang. Dropedge: Towards deep graph convolutional networks on node classification. *ArXiv*, 2019.

[23] Michael Scholkemper, Xinyi Wu, Ali Jadbabaie, and Michael T. Schaub. Residual connections and normalization can provably prevent oversmoothing in gnns. In *NeurIPS*, 2025.

[24] Xinyi Wu, Zhengdao Chen, William Wang, and Ali Jadbabaie. A non-asymptotic analysis of oversmoothing in graph neural networks. In *ICLR*, 2023.

[25] Guodong Shi, Claudio Altafini, and John S Baras. Dynamics over signed networks. *SIAM Review*, 2019.

[26] Dorwin Cartwright and Frank Harary. Structural balance: a generalization of heider's theory. *Psychological review*, 1956.

[27] Anton Tsitsulin, John Palowitch, Bryan Perozzi, and Emmanuel Müller. Graph clustering with graph neural networks. *Journal of Machine Learning Research*, 2023.

[28] Yunchong Song, Chenghu Zhou, Xinbing Wang, and Zhouhan Lin. Ordered gnn: Ordering message passing to deal with heterophily and over-smoothing. *arXiv preprint arXiv:2302.01524*, 2023.

[29] Yujun Yan, Milad Hashemi, Kevin Swersky, Yaoqing Yang, and Danai Koutra. Two sides of the same coin: Heterophily and oversmoothing in graph convolutional neural networks. In *ICDM*, 2022.

[30] Yuelin Wang, Kai Yi, Xinliang Liu, Yu Guang Wang, and Shi Jin. ACMP: Allen-cahn message passing with attractive and repulsive forces for graph neural networks. In *ICLR*, 2022.

[31] Eli Chien, Jianhao Peng, Pan Li, and Olgica Milenkovic. Adaptive universal generalized pagerank graph neural network. *arXiv preprint arXiv:2006.07988*, 2020.

[32] Langzhang Liang, Sunwoo Kim, Kijung Shin, Zenglin Xu, Shirui Pan, and Yuan Qi. Sign is not a remedy: Multiset-to-multiset message passing for learning on heterophilic graphs. *arXiv preprint arXiv:2405.20652*, 2024.

[33] Tyler Derr, Yao Ma, and Jiliang Tang. Signed graph convolutional networks. In *ICDM*, 2018.

[34] Yash Deshpande, Andrea Montanari, Elchanan Mossel, and Subhabrata Sen. Contextual stochastic block models. In *NeurIPS*, 2018.

[35] Jimmy Lei Ba, Jamie Ryan Kiros, and Geoffrey E Hinton. Layer normalization. *ArXiv*, 2016.

[36] Oleg Platonov, Denis Kuznedelev, Michael Diskin, Artem Babenko, and Liudmila Prokhorenkova. A critical look at the evaluation of gnns under heterophily: Are we really making progress? *arXiv preprint arXiv:2302.11640*, 2023.

[37] Andrew Kachites McCallum, Kamal Nigam, Jason Rennie, and Kristie Seymore. Automating the construction of internet portals with machine learning. *Information Retrieval*, 2000.

[38] C Lee Giles, Kurt D Bollacker, and Steve Lawrence. CiteSeer: An automatic citation indexing system. In *Proceedings of the third ACM conference on Digital libraries*, 1998.

[39] Kathi Canese and Sarah Weis. PubMed: the bibliographic database. *The NCBI handbook*, 2013.

[40] Weihua Hu, Matthias Fey, Marinka Zitnik, Yuxiao Dong, Hongyu Ren, Bowen Liu, Michele Catasta, and Jure Leskovec. Open graph benchmark: Datasets for machine learning on graphs. *arXiv preprint arXiv:2005.00687*, 2020.

- [41] Sergey Ioffe and Christian Szegedy. Batch normalization: Accelerating deep network training by reducing internal covariate shift. In *ICML*, 2015.
- [42] Johannes Gasteiger, Aleksandar Bojchevski, and Stephan Günnemann. Predict then propagate: Graph neural networks meet personalized pagerank. *ArXiv*, 2018.
- [43] Yifei Wang, Qi Zhang, Tianqi Du, Jiansheng Yang, Zhouchen Lin, and Yisen Wang. A message passing perspective on learning dynamics of contrastive learning. In *ICLR*, 2022.
- [44] Yifei Wang, Yisen Wang, Jiansheng Yang, and Zhouchen Lin. Dissecting the diffusion process in linear graph convolutional networks. In *NeurIPS*, 2021.
- [45] Ming Chen, Zhewei Wei, Zengfeng Huang, Bolin Ding, and Yaliang Li. Simple and deep graph convolutional networks. In *ICML*, 2020.
- [46] Moshe Eliasof, Lars Ruthotto, and Eran Treister. Improving graph neural networks with learnable propagation operators. In *International Conference on Machine Learning*, 2022.
- [47] Sitao Luan, Chenqing Hua, Qincheng Lu, Jiaqi Zhu, Mingde Zhao, Shuyuan Zhang, Xiaoming Chang, and Doina Precup. Revisiting heterophily for graph neural networks. *ArXiv*, 2022.
- [48] Moshe Eliasof, Eldad Haber, and Eran Treister. Pde-gcn: Novel architectures for graph neural networks motivated by partial differential equations. In *Neural Information Processing Systems*, 2021.
- [49] T Konstantin Rusch, Michael M Bronstein, and Siddhartha Mishra. A survey on oversmoothing in graph neural networks. *ArXiv*, 2023.

Appendix

Contents

A Limitations	14
B Background on GNNs	14
B.1 Graph Convolution Networks	14
B.2 Simplified Graph Convolution Networks	14
B.3 Signed Graph Propagation	14
C Proof of Theorem 3.2	15
D Proof of Theorem 4.2	16
E A Signed Graph Perspective on Existing Oversmoothing Countermeasures	17
E.1 Normalizations	18
E.2 Dropping	20
E.3 Residual Connections	20
F Oversmoothing Metrics	21
G Weakly Structural Balance	22
H Statement and Proof of Label-SBP	22
I Details of Experiments	24
I.1 Details of the Dataset	24
I.2 Experiments Setup	25
I.3 Time Complexity Analysis and the Modified SBP	25
I.4 Results Analysis	26
I.4.1 CSBM results	26
I.4.2 GCN Results	26
I.4.3 β Analysis on Heterophilic Datasets	27
I.4.4 SBP on more benchmarks	27
I.4.5 Different Backbones	28
I.4.6 SBP on Large-scale graphs	28
I.4.7 Further Optimization	28

A Limitations

This work evaluates a wide range of GNNs. However, due to the diversity of GNN methods, it is impractical to assess all of them. Therefore, the proposed method focuses on classic techniques that utilize normalization, dropout, and residual connections. Moreover, due to limited computational resources and time, the proposed method has not been evaluated on super-large graphs, such as those with 1G nodes. SBP focuses on the oversmoothing problem, which leads to degraded performance in GNNs. Other factors that can negatively impact GNN performance are not discussed in this paper.

B Background on GNNs

B.1 Graph Convolution Networks

To deal with non-Euclidean graph data, Graph Convolution Networks (GCNs) are proposed for direct convolution operation over graph, and have drawn interests from various domains. GCN is firstly introduced for a spectral perspective [8], but soon it becomes popular as a general message-passing algorithm in the spatial domain. In the feature transformation stage, GCN adopts a non-linear activation function (e.g., ReLU) and a layer-specific learnable weight matrix W for transformation. The propagation rule of GCN can be formulated as follows:

$$H_{(k)} = \text{ReLU}((\hat{A}H_{(k-1)})W_{(k)}) \quad (6)$$

B.2 Simplified Graph Convolution Networks

Simplified Graph Convolution Networks (SGC [9]) simplifies and separates the two stages of GCNs: feature propagation and (non-linear) feature transformation. It finds that utilizing only a simple logistic regression after feature propagation (removing the non-linearities), which makes it a linear GCN, can obtain comparable performance to canonical GCNs. The propagation rule of GCN can be formulated as follows:

$$H_{(k)} = \hat{A}H_{(k-1)}W_{(k)} = \hat{A}^k H_{(0)}W_{(k)} \dots W_{(1)} \quad (7)$$

Moreover, SGC transforms $W_{(k)} \dots W_{(1)}$ to a general learnable parameter W , so the formula of SGC can be this:

$$H_{(k)} = \hat{A}^k H_{(0)}W \quad (8)$$

B.3 Signed Graph Propagation

Classical GNNs [8, 9, 10, 11] primarily focused on message-passing on unsigned graphs or graphs composed solely of positive edges. For example, if there exists an edge $\{i, j\}$ or the sign of edge $\{i, j\}$ is positive, the node x_i updates its value by:

$$\hat{x}_i = x_i + \alpha(x_j - x_i) = (1 - \alpha)x_i + \alpha x_j, \alpha \in (0, 1). \quad (9)$$

Compared to the unsigned graph, a signed graph extends the edges to either positive or negative. Notably, if the sign of edge $\{i, j\}$ is negative, the node x_i updates its value using the following expression:

$$\hat{x}_i = x_i - \beta(x_j - x_i) = (1 + \beta)x_i - \beta x_j, \beta \in (0, 1). \quad (10)$$

In words, the positive interaction equation 9 indicates the attraction while the negative interaction equation 10 indicates that the nodes will repel their neighbors.

More generally, when considering all of the neighbors of node x_i , let N_i^+ denote the positive neighbor set while N_i^- denote the negative neighbor set, where $N_i^+ \cup N_i^- = N_i$ and $N_i^+ \cap N_i^- = \emptyset$. The representation of x_i is thus updated by:

$$\hat{x}_i = (1 - \alpha + \beta)x_i + \frac{\alpha}{|N_i^+|} \sum_{j \in N_i^+} x_j - \frac{\beta}{|N_i^-|} \sum_{j \in N_i^-} x_j. \quad (11)$$

In particular, the two parameters α and β mark the strength of positive and negative edges, respectively.

For further proofs of the theorems and propositions in the paper, we give a more simple and detailed definition in this section.

Let $D_{G^+} = \text{diag}(\deg_1^+, \dots, \deg_n^+)$ and $D_{G^-} = \text{diag}(\deg_1^-, \dots, \deg_n^-)$ be the degree matrices of the positive subgraph and negative subgraph, respectively. Let A_{G^+} be the adjacency matrix of the graph G^+ with $[A_{G^+}]_{ij} = 1$ if $\{i, j\} \in E^+$ and $[A_{G^+}]_{ij} = 0$ otherwise. The adjacency matrix A_{G^-} of the negative subgraph G^- is defined by $[A_{G^-}]_{ij} = -1$ for $\{i, j\} \in E^-$ and $[A_{G^-}]_{ij} = 0$ for $\{i, j\} \notin E^-$.

The Laplacian plays a central role in the algebraic representation of structural properties of graphs. In the presence of negative edges, more than one definition of Laplacian is possible; see [25]. The Laplacian of the positive subgraph G^+ is $L_{G^+} := D_{G^+} - A_{G^+}$, while for the negative subgraph G^- the following two variants can be used: $L_{G^-}^o := D_{G^-} - A_{G^-}$ and $L_{G^-}^r := -D_{G^-} - A_{G^-}$. Consequently, we have the following definitions.

Definition 1. Given the signed graph G , its opposing Laplacian is defined as

$$L_G^o := L_{G^+} + L_{G^-}^o = D_{G^+} + D_{G^-} - A_{G^+} - A_{G^-}, \quad (12)$$

and its repelling Laplacian is defined as

$$L_G^r = L_{G^+} + L_{G^-}^r = D_{G^+} - D_{G^-} - A_{G^+} - A_{G^-}. \quad (13)$$

Time is slotted at $t = 0, 1, \dots$. Each node i holds a state $x_i(t) \in \Omega$ at time t and interacts with its neighbors at each time to revise its state. The interaction rule is specified by the sign of the links. Let $\alpha, \beta \geq 0$. We first focus on a particular link $\{i, j\} \in E$ and specify for the moment the dynamics along this link isolating all other interactions.

The DeGroot Rule:

$$x_s(t+1) = x_s(t) + \alpha(x_{-s}(t) - x_s(t)) = (1 - \alpha)x_s(t) + \alpha x_{-s}(t), \quad (14)$$

where $-s \in \{i, j\} \setminus \{s\}$ with $\alpha \in (0, 1)$

The Opposing Rule:

$$x_s(t+1) = x_s(t) + \beta(-x_{-s}(t) - x_s(t)) = (1 - \beta)x_s(t) - \beta x_{-s}(t); \quad (15)$$

or The Repelling Rule:

$$x_s(t+1) = x_s(t) - \beta(x_{-s}(t) - x_s(t)) = (1 + \beta)x_s(t) - \beta x_{-s}(t). \quad (16)$$

The Repelling Negative Dynamics:

$$\begin{aligned} x_i(t+1) &= x_i(t) + \alpha \sum_{j \in N_i^+} (x_j(t) - x_i(t)) - \beta \sum_{j \in N_i^-} (x_j(t) - x_i(t)) \\ &= (1 - \alpha \deg_i^+ + \beta \deg_i^-) x_i(t) + \alpha \sum_{j \in N_i^+} x_j(t) - \beta \sum_{j \in N_i^-} x_j(t). \end{aligned} \quad (17)$$

Denote $\mathbf{x}(t) = (x_1(t) \dots x_n(t))^T$. We can now rewrite 17 in the compact form

$$\mathbf{x}(t+1) = M_G \mathbf{x}(t) = (I - \alpha L_{G^+} - \beta L_{G^-}^r) \mathbf{x}(t). \quad (18)$$

Here,

$$M_G = I - \alpha L_{G^+} - \beta L_{G^-}^r = I - L_G^{rw}, \quad (19)$$

with $L_G^{rw} = \alpha L_{G^+} + \beta L_{G^-}^r$ being the repelling weighted Laplacian of G . From Equation 18, $M_G \mathbf{1} = \mathbf{1}$ always holds. We present the following result, which by itself is merely a straightforward look into the spectrum of the repelling Laplacian L_G^{rw} .

C Proof of Theorem 3.2

Now consider the combined theorem.

Theorem C.1 Suppose that the positive edges are connected. Then along Equation 17 for any $0 < \alpha < 1 / \max_{i \in V} \deg_i^+$, there exists a critical value $\beta_* \geq 0$ for β such that

- (i) if $\beta < \beta_*$, then we have $\lim_{t \rightarrow \infty} x_i(t) = \sum_{j=1}^n x_j(0)/n$ for all initial values $x(0)$;
- (ii) if $\beta > \beta_*$, then $\lim_{t \rightarrow \infty} \|x(t)\| = \infty$ for almost all initial values w.r.t. Lebesgue measure.

Proof. we change the signed graph update to the equivalent version of $x_i(t)$ read as:

$$x_i(t+1) = x_i(t) + \alpha \sum_{j \in N_i^+} (x_j(t) - x_i(t)) - \beta \sum_{j \in N_i^-} (x_j(t) - x_i(t)).$$

This can be expressed as:

$$x(t+1) = (1 - \alpha \deg^+ + \beta \deg^-) x(t) + \alpha \sum_{j \in N^+} x_j(t) - \beta \sum_{j \in N^-} x_j(t). \quad (20)$$

Algorithm 20 can be written as:

$$x(t+1) = M_G x(t) = (I - \alpha L_G^+ - \beta L_G^-) x(t). \quad (21)$$

Here, $M_G = I - \alpha L_G^+ - \beta L_G^-$, with $L_G^+ = \alpha L_G^+ + \beta L_G^-$ being the repelling weighted Laplacian of G , defined in Sec.B.3. From Eq.equation 21, $M_G \mathbf{1} = \mathbf{1}$ always holds. We present the following result, which by itself is merely a straightforward look into the spectrum of the repelling Laplacian L_G^- .

So theorem C.1 can be changed to the following version:

Suppose G^+ is connected. Then along Eq.equation 21 for any $0 < \alpha < 1 / \max_{i \in V} \deg_i^+$, there exists a critical value $\beta > 0$ for β such that:

- (i) if $\beta < \beta_*$, then average consensus is reached in the sense that $\lim_{t \rightarrow \infty} x_i(t) = \frac{1}{n} \sum_{j=1}^n x_j(0)$ for all initial values $x(0)$;
- (ii) if $\beta > \beta_*$, then $\lim_{t \rightarrow \infty} \|x(t)\| = \infty$ for almost all initial values w.r.t. Lebesgue measure.

Proof. Define $J = 11^T / n$. Fix $\alpha \in (0, 1 / \max_{i \in V} \deg_i^+)$ and consider $f(\beta) = \lambda_{\max}(I - \alpha L_G^+ - \beta L_G^- - J)$, and $g(\beta) = \lambda_{\min}(I - \alpha L_G^+ - \beta L_G^- - J)$. The Courant–Fischer Theorem implies that both $f(\cdot)$ and $g(\cdot)$ are continuous and nondecreasing functions over $[0, \infty)$. The matrix J always commutes with $I - \alpha L_G^+ - \beta L_G^-$, and 1 is the only nonzero eigenvalue of J . Moreover, the eigenvalue 1 of J shares a common eigenvector 1 with the eigenvalue 1 of $I - \alpha L_G^+ - \beta L_G^-$.

Since G^+ is connected, the second smallest eigenvalue of L_{G^+} is positive. Since $0 < \alpha < \frac{1}{\max_{i \in V} \deg_i^+}$, there holds $\lambda_{\min}(I - \alpha L_{G^+}) \geq -1$, again due to the Gershgorin Circle Theorem. Therefore, $f(0) < 1$, $g(0) \geq -1$. Noticing $f(\infty) = \infty > 1$, there exists $\beta_* > 0$ satisfying $f(\beta_*) = 1$. We can then verify the following facts:

- There hold $f(\beta) < 1$ and $g(\beta) > -1$ if $\beta < \beta_*$. In this case, along Eq.equation 21 $\lim_{t \rightarrow \infty} (I - J)x(t) = 0$, which in turn implies that $x(t)$ converges to the eigenspace corresponding to the eigenvalue 1 of M_G . This leads to the average consensus statement in (i).
- There holds $f(\beta) \geq 1$ if $\beta > \beta_*$. In this case, along Eq.equation 21 $x(t)$ diverges as long as the initial value $x(0)$ has a nonzero projection onto the eigenspace corresponding to $\lambda_{\max}(M_G)$ of M_G . This leads to the almost everywhere divergence statement in (ii).

The proof is now complete.

D Proof of Theorem 4.2

Theorem D.1 let $A > 0$ be a constant and define $\mathcal{F}(z)_c$ by $\mathcal{F}(z)_c = -c, z < -c$, $\mathcal{F}(z)_c = z, z \in [-c, c]$, and $\mathcal{F}(z)_c = c, z > c$. Define the function $\theta : E \rightarrow \mathbb{R}$ so that $\theta(\{i, j\}) = \alpha$ if $\{i, j\} \in E^+$ and $\theta(\{i, j\}) = -\beta$ if $\{i, j\} \in E^-$. Assume that node i interacts with node j at time t and consider the following node interaction under the signed propagation rules:

$$x_s(t+1) = \mathcal{F}(z)_c((1 - \theta)x_s(t) + \theta x_{-s}(t)), \quad s \in \{i, j\}. \quad (22)$$

let $\alpha \in (0, 1/2)$. Assume that G is a structurally balanced complete graph under the partition $V = V_1 \cup V_2$. When β is sufficiently large, for almost all initial values $x(0)$ w.r.t. Lebesgue measure, there exists a binary random variable $l(x(0))$ taking values in $\{-c, c\}$ such that

$$\mathbb{P} \left(\lim_{t \rightarrow \infty} x_i(t) = l(x(0)), i \in V_1; \lim_{t \rightarrow \infty} x_i(t) = -l(x(0)), i \in V_2 \right) = 1. \quad (23)$$

Proof. The proof is based on the following lemmas.

Lemma D.2 Fix $\alpha \in (0, 1)$ with $\alpha \neq \frac{1}{2}$. For the dynamics 22 with the random pair selection process, there exists $\beta^*(\alpha) > 0$ such that

$$\mathbb{P} \left(\limsup_{t \rightarrow \infty} \max_{i, j \in V} |x_i(t) - x_j(t)| = 2A \right) = 1$$

for almost all initial beliefs if $\beta > \beta^*$.

Lemma D.3 Fix $\alpha \in (1/2, 1)$ and $\beta \geq 2/(2\alpha - 1)$. Consider the dynamics 22 with the random pair selection process. Let G be the complete graph with $\kappa(G^+) \geq 2$. Suppose for time t there are $i_1, j_1 \in V$ with $x_{i_1}(t) = -c$ and $x_{j_1}(t) = c$. Then for any $\epsilon \in [0, (2\alpha - 1)c/2\alpha]$ and any $i_* \in V$, the following statements hold:

- (i) There exist an integer $Z(\epsilon)$ and a sequence of node pair realizations, $G_{t+s}(\omega)$, for $s = 0, 1, \dots, Z - 1$, under which $x_{i_*}(t + Z)(\omega) \leq -A + \epsilon$.
- (ii) There exist an integer $Z(\epsilon)$ and a sequence of node pair realizations, $G_{t+s}(\omega)$, for $s = 0, 1, \dots, Z - 1$, under which $x_{i_*}(t + Z)(\omega) \geq A - \epsilon$.

Proof. From our standing assumption, the negative graph G^- contains at least one edge. Let $k_*, m_* \in V$ share a negative link. We assume the two nodes $i_1, j_1 \in V$ labeled in the lemma are different from k_*, m_* , for ease of presentation. We can then analyze all possible sign patterns among the four nodes i_1, j_1, k_*, m_* . We present here just the analysis for the case with

$$\{i_1, k_*\} \in E^+, \{i_1, m_*\} \in E^+, \{j_1, k_*\} \in E^+, \{j_1, m_*\} \in E^+.$$

The other cases are indeed simpler and can be studied via similar techniques.

Without loss of generality we let $x_{m_*}(t) \geq x_{k_*}(t)$. First of all we select $G_t = \{i_1, k_*\}$ and $G_{t+1} = \{j_1, m_*\}$. It is then straightforward to verify that

$$x_{m_*}(t+2) \geq x_{k_*}(t+2) + 2\alpha c.$$

By selecting $G_{t+2} = \{m_*, k_*\}$ we know from $\beta \geq \frac{2}{(2\alpha-1)} > \frac{1}{\alpha}$ that

$$x_{k_*}(t+3) = -c, \quad x_{m_*}(t+3) = c.$$

There will be two cases:

- (a) Let $i_* \in \{m_*, k_*\}$. Noting that $\kappa(G^+) \geq 2$, there will be a path connecting to k_* from i_* without passing through m_* in G^+ . It is then obvious that we can select a finite number Z_1 of links which alternate between $\{m_*, k_*\}$ and the edges over that path so that $x_{i_*}(t+3+Z_1) \geq -c + \epsilon$. Here Z_1 depends only on α and n .
- (b) Let $i_* \in \{m_*, k_*\}$. We only need to show that we can select pair realizations so that x_{m_*} can get close to $-c$, and x_{k_*} gets close to c after $t+3$. Since G^+ is connected, either m_* or k_* has at least one positive neighbor. For the moment assume m' is a positive neighbor of m_* and k' is a positive neighbor of k_* with $m' \neq k'$. Then from part (a) we can select Z_2 node pairs so that

$$x_{m_*}(t+3+Z_2) \leq -c + \epsilon, \quad x_{k_*}(t+3+Z_2) \geq c - \epsilon.$$

Thus, selecting the negative edge $\{m_*, k_*\}$ for $t+5+Z_2$ implies $x_{m_*}(t+6+Z_2) = c$ for $\beta \geq \frac{2}{(2\alpha-1)}$. The case with $m' = k'$ can be dealt with by a similar treatment, leading to the same conclusion.

This concludes the proof of the lemma.

In view of Lemmas D.2 and D.3, the desired theorem is a consequence of the second Borel–Cantelli Lemma.

E A Signed Graph Perspective on Existing Oversmoothing Countermeasures

We defined the signed graph propagation over the whole graph \mathcal{G} written in the matrix form as:

$$\hat{X} = (1 - \alpha + \beta)X + \alpha \hat{A}^+ X - \beta \hat{A}^- X, \quad (24)$$

Table 5: The mathematically equivalent raw normalized positive and negative adjacency matrices in signed graph propagation of various anti-oversmoothing methods.

Method	Characteristic	Positive \hat{A}^+	Negative \hat{A}^-
GCN	K -layer graph convolutions	\hat{A}	0
SGC	K -layer linear graph convolutions	\hat{A}	0
BatchNorm	Normalized with column means and variance	\hat{A}	$\mathbb{1}_n \mathbb{1}_n^T / n \hat{A}$
PairNorm	Normalized with the overall means and variance	\hat{A}	$\mathbb{1}_n \mathbb{1}_n^T / n \hat{A}$
ContraNorm	Uniformed norm derived from contrastive loss	\hat{A}	$(XX^T)\hat{A}$
DropEdge	Randomized augmentation	\hat{A}	\hat{A}_m
Residual	Last layer connection	\hat{A}	I
APPNP	Initial layer connection	$\sum_{i=0}^{k+1} \alpha^i \hat{A}^i$	$\alpha \sum_{j=0}^k \alpha^j \hat{A}^j$
JKNET	Jumping to the last layer	$\sum_{i=0}^k \alpha^i \hat{A}^i + \hat{A}^{k+1}$	$\sum_{j=0}^k \alpha^j \hat{A}^k$
DAGNN	Adaptively incorporating different layer	$\sum_{i=0}^k \alpha^i \hat{A}^i + \hat{A}^{k+1}$	$\sum_{j=0}^k \alpha^j \hat{A}^k$
Feature-SBP (ours)	Label-induced negative graph	\hat{A}	$\text{softmax}(A_f^-)$
Label-SBP (ours)	Feature-induced negative graph	\hat{A}	$\text{softmax}(A_l^-)$

where \hat{A}^+ is the raw normalized version of the positive adjacency matrix $A^+ \in \{0, 1\}^{n \times n}$ and \hat{A}^- is that of the negative adjacency matrix $A^- \in \{0, 1\}^{n \times n}$.

We summarize eight specific methods with their corresponding positive and negative graphs in Table 5.

E.1 Normalizations

BatchNorm BatchNorm centers the node representations X to zero mean and unit variance and can be written as $\text{BatchNorm}(x_i) = \frac{1}{\sqrt{\sigma^2 + \epsilon}}(x_i - \frac{1}{n} \sum_{i=1}^n x_i)$, where $\epsilon > 0$ and σ^2 is the variance of node features. We rewrite BatchNorm in the signed graph propagation form as follows:

$$\hat{X} = \hat{A}X\Gamma_d^{-1} - \frac{\mathbb{1}_n \mathbb{1}_n^T}{n} \hat{A}X\Gamma_d^{-1} = \hat{A}\tilde{X} - \frac{\mathbb{1}_n \mathbb{1}_n^T}{n} \hat{A}\tilde{X}, \quad (25)$$

where $\Gamma_d = \text{diag}(\sigma_1, \dots, \sigma_d)$ is a diagonal matrix that represents column-wise variance with $\sigma_i^2 = \frac{1}{n} \sum_{j=1}^n ((\hat{A}X)_{ji} - \mathbb{1}_n^T \hat{A}X/n)^2$, and $\tilde{X} = X\Gamma_d^{-1}$ is a normalized version of X . We can correspond to the positive graph \hat{A}^+ to \hat{A} and the negative graph \hat{A}^- to $\frac{\mathbb{1}_n \mathbb{1}_n^T}{n} \hat{A}$ in equation 25.

PairNorm We then introduce another method called PairNorm where the only difference between it and BatchNorm is that PairNorm scales all the entries in X using the same number rather than scaling each column by its own variance. The formulation of PairNorm can be rewritten as follows:

$$\hat{X} = \frac{1}{\Gamma} \hat{A}X - \frac{1}{\Gamma} \frac{\mathbb{1}_n \mathbb{1}_n^T}{n} \hat{A}X = \frac{1}{\Gamma} (\hat{A}X - \frac{\mathbb{1}_n \mathbb{1}_n^T}{n} \hat{A}X), \quad (26)$$

where $\Gamma = \|(\hat{A} - \frac{\mathbb{1}_n \mathbb{1}_n^T}{n} \hat{A})X\|_F / \sqrt{n}$. We observe that PairNorm shares the same positive and negative graphs (up to scale) as BatchNorm. Another normalization technique, ContraNorm, turns out to extend the negative graph to an adaptive one based on node feature similarities.

Proposition E.1 Consider the update:

$$\hat{X} = \hat{A}X - \frac{\mathbb{1}_n \mathbb{1}_n^T}{n} \hat{A}X, \quad (27)$$

where $A \in \{0, 1\}^{n \times n}$ is the adjacency matrix. Define the overall signed graph adjacency matrix A_s as $A - \frac{\mathbb{1}_n \mathbb{1}_n^T}{n} A$. Then we have that the signed graph is (weakly) structurally balanced only if the original graph can be divided into several isolated complete subgraphs.

Proof. Assume that there is no isolated node and no node has edges with all the other nodes. $(A_s)_{i,j} = (A)_{i,j} - \frac{\deg_j}{n}$. If $(A)_{i,j} = 1$, then we have $(A_s)_{i,j} > 0$. If $(A)_{i,j} = 0$, then we have $(A_s)_{i,j} < 0$.

If the nodes can be divided into several isolated complete subgraphs, then the nodes set $V = V_1 \cup V_2 \dots V_m$, where $|V_i| > 1$, m is the number of the isolated complete subgraphs. So only the nodes within the same set have edges, thus relative entries of $A_s > 0$, while nodes from different sets do not, thus relative entries of $A_s < 0$.

On the other hand, if A_s is (weakly) structurally balanced, then the nodes set can be expressed as $V = V_1 \cup V_2 \dots V_k$, where $|V_i| > 1$, k is the number of the separated parties in the signed graph. The entry of A_s in the same parties is positive, while between different parties is negative. According to $(A_s)_{i,j} = (A)_{i,j} - \frac{\deg_j}{n}$, we know that nodes in the same parties are connected in the original graph while not connected in the original graph between different parties. So the graph can be divided into several isolated complete subgraphs.

Overall, the signed graph is (weakly) structurally balanced only if the original graph can be divided into several isolated complete subgraphs, the proof is over.

The Proposition shows that in order for the structural balance property to hold for the signed graph of normalization, the graph needs to satisfy an unrealistic condition where the edges strictly cluster the nodes.

ContraNorm ContraNorm is inspired by the uniformity loss from contrastive learning, aiming to alleviate dimensional feature collapse. For simplicity, we consider the spectral version of ContraNorm that takes the following form:

$$\hat{X} = (1 + \alpha) \hat{A}X - \alpha/\tau (\mathbf{X} \mathbf{X}^T) \hat{A}X, \quad (28)$$

where $\alpha \in (0, 1)$ and $\tau > 0$ are hyperparameters. We can see that \hat{A} is again the positive graph and $(\mathbf{X} \mathbf{X}^T) \hat{A}$ is the negative graph in the corresponding signed graph propagation.

Consider the update:

$$\hat{X} = \hat{A}X - \frac{\mathbf{X} \mathbf{X}^T}{n} \hat{A}X, \quad (29)$$

Define the overall signed graph adjacency matrix $A_s = A - \frac{\mathbf{X} \mathbf{X}^T}{n} A$ where $(A_s)_{i,j} = (A)_{i,j} - \frac{1}{n} \sum_{k=1}^n x_i x_k^T (A)_{k,j}$.

Assume that the nodes feature is normalized every update, that is $\|x_i\|_2 = 1$ for every i .

If $(A)_{i,j} = 1$, then we have that

$$\begin{aligned} (A_s)_{i,j} &= (A)_{i,j} - \frac{1}{n} \sum_{k=1}^n x_i x_k^T (A)_{k,j} \\ &= 1 - \frac{1}{n} \sum_{k=1}^n x_i x_k^T (A)_{k,j} \\ &> 1 - \frac{1}{n} \sum_{k=1}^n (A)_{k,j} \\ &= 1 - \frac{d_j}{n} > 0. \end{aligned} \quad (30)$$

That means if $(A)_{i,j} = 1$, then $(A_s)_{i,j} > 0$. However, if $(A)_{i,j} = 0$, then we have that

$$\begin{aligned} (A_s)_{i,j} &= (A)_{i,j} - \frac{1}{n} \sum_{k=1}^n x_i x_k^T (A)_{k,j} \\ &= -\frac{1}{n} \sum_{k=1}^n x_i x_k^T (A)_{k,j} \\ &= -\frac{1}{n} \sum_{k \in N_j} x_i x_k^T. \end{aligned} \quad (31)$$

Intuitively, if x_i has similar features to x_j 's neighbors, then we have that $(A_s)_{i,j} < 0$, which means trying to repel nodes with similar representations. If x_i has different features to x_j 's neighbors,

then we have that $(A_s)_{i,j} > 0$, which means trying to aggregate nodes with original different representations.

If graph G is a completed graph, then all entries of $(A_s) > 0$, however, when all of the nodes coverage to each other, $\sum_{k=1}^n x_i x_k^T (A)_{k,j} = \sum_{k=1}^n x_i x_k^T$ will also become bigger.

E.2 Dropping

For DropMessage [21], it is a unified way of DropNode, DropEdge and Dropout but with a more flexible mask strategy. We have discussed the DropNode and DropEdge in our paper. DropMessage can be viewed as randomly dropping some dimension of the aggregated node features instead of the whole node or the whole edge. We give the unified positive and negative graph of DropMessage in the term of the signed graph. The propagation of DropMessage can be expressed as $H^{(k)} = AH^{(k-1)} - M_m$, where if dropping $AH_{ij}^{(k-1)}$, then $M_{ij} = AH_{ij}^{(k-1)}$ else $M_{ij} = 0$.

E.3 Residual Connections

The standard residual connection [44, 45] directly combines the previous and the current layer features together. It can be formulated as:

$$\hat{X} = (1 - \alpha)X + \alpha \hat{A}X = X + \alpha \hat{A}X - \alpha \mathcal{I}X. \quad (32)$$

For residual connections, the positive adjacency matrix is \hat{A} and the negative adjacency matrix \mathcal{I} in the corresponding signed graph propagation.

APPNP We reformulate the method APPNP [42] as the signed propagation form of the initial node feature. Another propagation process is APPNP [42] which can be viewed as a layer-wise graph convolution with a residual connection to the initial transformed feature matrix $X^{(0)}$, expressed as:

$$\hat{X}^{(k+1)} = (1 - \alpha)X^{(0)} + \alpha \hat{A}X^{(k)}. \quad (33)$$

Theorem E.2 *With $\hat{A}^+ = \sum_{i=0}^{k+1} \alpha^i \hat{A}^i$ and $\hat{A}^- = \alpha \sum_{j=0}^k \alpha^j \hat{A}^j$, the propagation process of APPNP following the signed graph propagation.*

Proof. Easily prove with mathematical induction.

In addition to combining with the last and initial layer features, the last type integrates several intermediate layer features. The established representations are JKNET [18] and DAGNN [19].

JKNET JKNET is a deep graph neural network which exploits information from neighborhoods of differing locality. JKNET selectively combines aggregations from different layers with Concatenation/Max-pooling/Attention at the output, i.e., the representations "jump" to the last layer. Using attention mechanism for combination at the last layer, the $k + 1$ -layer propagation result of JKNET can be written as:

$$\begin{aligned} X^{(k+1)} &= \alpha_0 X^{(0)} + \alpha_1 X^{(1)} + \cdots + \alpha_k X^{(k)} \\ &= \sum_{i=0}^k \alpha_i \hat{A}^i X^{(0)}, \end{aligned} \quad (34)$$

where $\alpha_0, \alpha_1, \dots, \alpha_k$ are the learnable fusion weights with $\sum_{i=0}^k \alpha_i = 1$.

DAGNN Deep Adaptive Graph Neural Networks (DAGNN) [19] tries to adaptively add all the features from the previous layer to the current layer features with the additional learnable coefficients. After decoupling representation transformation and propagation, the propagation mechanism of DAGNN is similar to that of JKNET.

$$X^{(k+1)} = \sum_{i=0}^k \alpha_i \hat{A}^i H^{(0)}, H^{(0)} = f_\theta(X^{(0)}) \quad (35)$$

$H^{(0)} = f_\theta(X^{(0)})$ is the non-linear feature transformation using an MLP network, which is conducted before the propagation process and $\alpha_0, \alpha_1, \dots, \alpha_k$ are the learnable fusion weights with $\sum_{i=0}^k \alpha_i = 1$.

Theorem E.3 With $\hat{A}^+ = \sum_{i=0}^{k-1} \alpha^i \hat{A}^i + \hat{A}^k$ and $\hat{A}^- = \sum_{j=0}^{k-1} \alpha^j \hat{A}^k$, the propagation process of JKNET and DAGNN following the signed graph propagation.

Proof. Easily prove with mathematical induction.

As for more residual inspired methods [20, 46, 47, 48], we select GCNII and wGCN to give a detailed discussion as follows.

- As for GCNII [20], it is an improved version of APPNP with the learnable coefficients α_i and changes the learnable weight W to $(1 - \beta_i)I + \beta_i W$ each layer, so it shares the same positive and negative graph as APPNP.
- As for the wGCN [46], it incorporates trainable channel-wise weighting factors ω to learn and mix multiple smoothing and sharpening propagation operators at each layer, same as the init residual combines but change parameters α to be learnable with a more detailed selection strategy.

F Oversmoothing Metrics

There exist a variety of different approaches to quantify over-smoothing in deep GNNs, here we choose the measure based on the Dirichlet energy on graphs [15, 49].

$$\epsilon(X(t)) = \frac{1}{v} \sum_{i \in V} \sum_{j \in N_i} \|x_i(t) - x_j(t)\|_2^2, \quad (36)$$

where v is the number of the nodes, $x_i(t)$ is the node feature of node i at time t . N_i represents the neighbor set of node i , In the signed graph, it including nodes connected to i by both positive and negative edges. Oversmoothing means that when the layers are infinity, all of the node features will converge, that is to say $\lim_{t \rightarrow \infty} \epsilon(X(t)) \rightarrow 0$.

In Theorem 3.2, there are 2 cases:

- if $\beta < \beta_*$, then we have $\lim_{t \rightarrow \infty} x_i(t) = \sum_{j=1}^n x_j(0)/n$ for all initial values $x(0)$
- if $\beta > \beta_*$, then $\lim_{t \rightarrow \infty} \|x(t)\| = \infty$ for almost all initial values w.r.t. Lebesgue measure.

In the first case, all the node features will coverage to the mean of them and therefore $\lim_{t \rightarrow \infty} \epsilon(X(t)) \rightarrow 0$, then oversmoothing happens. In the second case, the node features will diverge to infinity and thus $\lim_{t \rightarrow \infty} \epsilon(X(t)) \rightarrow 0$ or ∞ which is also not what we want.

Theorem 3.2 demonstrated that both insufficient repulsion and excessive repulsion caused by the negative graph can hinder performance in signed graph propagation. From this, we conclude that relying solely on the negative signs is insufficient to alleviate oversmoothing. Therefore, we propose the provable solution: a structurally balanced graph to efficiently alleviate oversmoothing in Theorem 4.2. Specifically, we have the following conclusion from the structurally balanced graph in Theorem 4.2:

$$\mathbb{P} \left(\lim_{t \rightarrow \infty} x_i(t) = l(x(0)), i \in V_1; \lim_{t \rightarrow \infty} x_i(t) = -l(x(0)), i \in V_2 \right) = 1. \quad (37)$$

Then we have:

$$\lim_{t \rightarrow \infty} \epsilon(X(t)) = \lim_{t \rightarrow \infty} \frac{1}{v} \sum_{i \in V} \sum_{j \in N_i} \|x_i(t) - x_j(t)\|_2^2 \quad (38)$$

$$= \lim_{t \rightarrow \infty} \frac{1}{v} \sum_{i \in V_1} \sum_{j \in N_i} \|x_i(t) - x_j(t)\|_2^2 + \frac{1}{v} \sum_{i \in V_2} \sum_{j \in N_i} \|x_i(t) - x_j(t)\|_2^2 \quad (39)$$

$$= \lim_{t \rightarrow \infty} \frac{1}{v} \sum_{i \in V_1} \sum_{j \in N_i, y_i \neq y_j} \|x_i(t) - x_j(t)\|_2^2 + \frac{1}{v} \sum_{i \in V_2} \sum_{j \in N_i, y_i \neq y_j} \|x_i(t) - x_j(t)\|_2^2 \quad (40)$$

$$= \lim_{t \rightarrow \infty} \frac{1}{v} \sum_{i \in V_1} \frac{v}{2} \times 2c + \frac{1}{v} \sum_{i \in V_2} \frac{v}{2} \times 2c \quad (41)$$

$$= \lim_{t \rightarrow \infty} \frac{1}{v} \left(\frac{v}{2} \times \frac{v}{2} \times 2c + \frac{v}{2} \times \frac{v}{2} \times 2c \right) \quad (42)$$

$$= vc \geq 0 \quad (43)$$

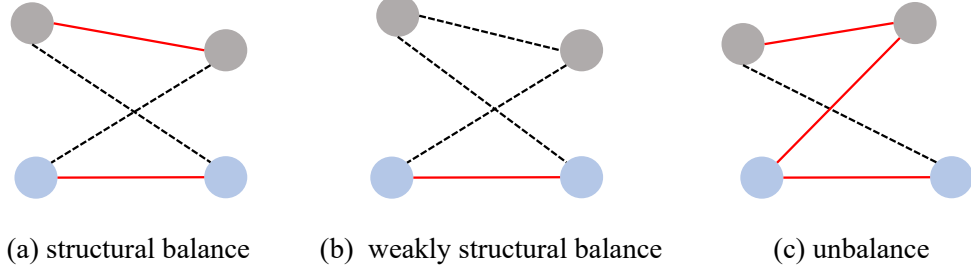


Figure 7: Examples of structural balanced (left), weakly structural balanced (middle), and unbalanced signed graphs (right). Here red lines represent positive edges; black dashed lines represent negative edges; gray and blue circles represent nodes from different labels

So Theorem 4.2 proves that under certain conditions, structural balance can alleviate oversmoothing even when the layers are infinity.

G Weakly Structural Balance

To clarify the concept of structural balance, weakly structural balance and unbalance signed graph, we give the examples as shown in Figure 7. The notion of structural balance can be weakened in the following definition G.1.

Definition G.1 A signed graph G is **weakly structurally balanced** if there is a partition of V into $V = V_1 \cup V_2 \cup \dots \cup V_m$, $m \geq 2$ with V_1, \dots, V_m being nonempty and mutually disjoint, where any edge between different V_i 's is negative, and any edge within each V_i is positive.

Then we show that when \mathcal{G} is a complete graph, weak structural balance also leads to clustering of node states.

Theorem G.2 ([25], Theorem 10) Assume that node i interacts with node j and $x_i(t)$ represents the value of node i at time t . Let $\theta = \alpha$ if the edge $\{i, j\}$ is positive and $\theta = \beta$ if the edge $\{i, j\}$ is negative. Consider the constrained signed propagation update:

$$x_i(t+1) = \mathcal{F}_c((1-\theta)x_i(t) + \theta x_j(t)). \quad (44)$$

Let $\alpha \in (0, 1/2)$. Assume that \mathcal{G} is a weakly structurally balanced complete graph under the partition $V = V_1 \cup V_2 \cup \dots \cup V_m$. When β is sufficiently large, for almost all initial values $x(0)$ w.r.t. Lebesgue measure, there exists m random variable $l_1(x(0)), l_2(x(0)), \dots, l_m(x(0))$, each of which taking values in $\{-c, c\}$ such that

$$\mathbb{P} \left(\lim_{t \rightarrow \infty} x_i(t) = l_j(x(0)), i \in V_j, j = 1, \dots, m \right) = 1. \quad (45)$$

H Statement and Proof of Label-SBP

In this section, we show that our method Label-SBP can create a structurally balanced graph under certain conditions and thus provably alleviate oversmoothing as the number of propagation steps increases. To achieve this, we introduce a metric, *structural imbalance degree* (SID), to quantify the level of structural balance in arbitrary signed graph. Specifically, SID counts the number of edges that must be changed to achieve the structural balance.

Definition H.1 (Structural Imbalance Degree) For each node v in a signed graph \mathcal{G}_s of n nodes, let $\mathcal{P}(v)$ denote the subset of nodes that has the same label as v but connected to v by a non-positive edge; let $\mathcal{N}(v)$ denote the subset of nodes that has a different label from v but connected

Table 6: \mathcal{SID} on CSBM (Contextual Stochastic Block Model) with different methods. We set the two class means $u_1 = -1$ and $u_2 = 1$ respectively, the number of nodes $N = 100$, intra-class edge probability $p = 2 \log 100/100$ and inter-class edge probability $q = \log 100/100$.

Method	\mathcal{P}_{\downarrow}	\mathcal{N}_{\downarrow}	$\mathcal{SID}_{\downarrow}$
DropEdge	92.62	100.00	96.31
Residual	90.87	100.00	95.44
GCN/SGC	89.87	100.00	94.94
APPNP	0.00	100.00	50.00
JKNET	0.00	100.00	50.00
DAGNN	0.00	100.00	50.00
BatchNorm	89.87	4.56	47.22
PairNorm	89.87	4.56	47.22
ContraNorm	89.87	4.56	47.22
Feature-SBP (ours)	89.87	4.56	47.22
Label-SBP (ours)	32.46	36.16	34.31

to v by a non-negative edge. Then the structural imbalance degree of \mathcal{G} is defined as $\mathcal{SID}(\mathcal{G}_s) = \frac{1}{2n} \sum_{v \in \mathcal{G}_s} (|\mathcal{P}(v)| + |\mathcal{N}(v)|)$.

\mathcal{SID} exhibits a fundamental characteristic: it increases as more edge signs deviate from the criteria of a structurally balanced graph, suggesting a higher degree of structural imbalance. Specifically, when the signed graph achieves the structural balance, we can assert that $\mathcal{SID} = 0$ as follows:

Proposition H.2 For a structural balanced complete graph \mathcal{G}_{sb} , we have $\mathcal{SID}(\mathcal{G}_{sb}) = 0$.

Proof If the graph is structurally balanced, we can see that for a node v , $\mathcal{P}(v) = 0$ and $\mathcal{N}(v) = 0$ due to the structural balance complete graph assumption. So $\mathcal{SID}(\mathcal{G}) = 0$.

Based on the \mathcal{SID} , we can quantify the degree of structural balance in the equivalent signed graphs induced by anti-oversmoothing methods discussed in the previous section, as shown in Table 6. Our results show that previous anti-oversmoothing methods either remain a high \mathcal{SID} or an imbalance \mathcal{P} and \mathcal{N} . In contrast, our methods effectively reduce the \mathcal{SID} , resulting in a more structurally balanced graph, or at least be on par with previous methods.

Besides the empirical observation, we present the following theoretical result which demonstrates that Label-SBP can be guaranteed to achieve a certain level of structure balance:

Proposition H.3 Assuming balanced node label classes with $|Y_1| = |Y_2|$, a labeled node ratio denoted as p , and the signed graph \mathcal{G}_s^l created by Label-SBP, then we have $\mathcal{SID}(\mathcal{G}_s^l) \leq (1 - p)n/2$.

Proof Without loss of generality, assume that the node feature has been normalized which means that $\|x_i\|_2 = 1$ for every i . If x_i and x_j has the same label, then we have that, $(A_s)_{i,j} = (A)_{i,j} + 1 > 1$. If x_i and x_j has different labels, then we have that $(A_s)_{i,j} = (A)_{i,j} - 1 \leq 0$.

We first prove that $\mathcal{SID}(\mathcal{G}, p) \leq (1 - p)\frac{n}{2}$ where n is the nodes number and p is the label ratio. We have that

$$\mathcal{P}(v) + \mathcal{N}(v) \leq (1 - p)n, \quad (46)$$

because for a single node v only the remaining $(1 - p)n$ nodes' labels are unknown and therefore their edges may need to change so that

$$\begin{aligned} \mathcal{SID}(\mathcal{G}) &= \frac{1}{2n} \sum_{v \in \mathcal{G}} (|\mathcal{P}(v)| + |\mathcal{N}(v)|) \\ &\leq \frac{1}{2n} \sum_{v \in \mathcal{G}} (1 - p)n \\ &= (1 - p)\frac{n}{2}. \end{aligned} \quad (47)$$

We know that when $\mathcal{SID}(\mathcal{G}) = 0$, then we have that the nodes V set can be divided into $V_1 \cup V_1 \dots \cup V_L$ where L is the number of the node classes. There are only positive edges with the node subset and only negative edges between the node subset.

Since $C = 2$, the node set can be divided into V_1 and V_2 , the signed graph is structurally balanced. According to Theorem 4.2, we have that the nodes in V_1 will converge to the c where $\|c\|_2 = 1$ and the nodes in V_2 will converge to $-c$. Thus under Label-SBP propagation, the oversmoothing will only happen within the same label and repel different labels to the boundary.

Proposition H.3 suggests that Label-SBP constrains \mathcal{SID} linearly with the training ratio p , indicating that \mathcal{SID} diminishes with an increase in the labeling ratio p . In particular, it implies that Label-SBP can strictly establish a structurally balanced graph for any graph under the full supervision condition, making the model easier to distinguish nodes with different labels as the number of layers increases:

Theorem H.4 *Under full supervision ($p = 1$), the signed graph $\hat{\mathcal{G}}_s^l$ induced by Label-SBP achieves $\mathcal{SID}(\hat{\mathcal{G}}_s^l) = 0$. Consequently, under the constrained signed propagation as given by equation 2, nodes from distinct classes will converge towards unique constants.*

$$\mathbb{P} \left(\lim_{k \rightarrow \infty} X_i^{(k)} = c, i \in \tilde{V}_1; \lim_{k \rightarrow \infty} X_i^{(k)} = -c, i \in \tilde{V}_2 \right) = 1. \quad (48)$$

I Details of Experiments

I.1 Details of the Dataset

Table 7: Summary of datasets. $H(G)$ refers to the edge homophily level: the higher, the more homophilic the dataset is.

Dataset	$H(G)$	Classes	Nodes	Edges
Cora	0.81	7	2,708	5,429
Citeseer	0.74	6	3,327	4,732
PubMed	0.80	3	19,717	44,338
Texas	0.21	5	183	295
Cornell	0.30	5	183	280
Amazon-ratings	0.38	5	24,492	93,050
Wisconsin	0.11	5	251	466
Squirrel	0.22	4	198,493	2,089
Ogbn-Arxiv	0.65	40	16,9343	1,166,243

We consider two types of datasets: Homophilic and Heterophilic. They are differentiated by the *homophily level* of a graph.

$$\mathcal{H} = \frac{1}{|V|} \sum_{v \in V} \frac{\text{Number of } v\text{'s neighbors who have the same label as } v}{\text{Number of } v\text{'s neighbors}}.$$

The low homophily level means that the dataset is more heterophilic when most of the neighbors are not in the same class, and the high homophily level indicates that the dataset is close to homophilic when similar nodes tend to be connected. In the experiments, we use four homophilic datasets, including Cora, CiteSeer, PubMed, and Ogbn-Arxiv, and four heterophilic datasets, including Texas, Wisconsin, Cornell, Squirrel, and Amazon-rating [36]). The datasets we used covers various homophily levels.

CSBM Settings. To quantify the structural balance of the mentioned methods, we simplified the graph to 2-CSBM($N, p, q, \mu_1, \mu_2, \sigma^2$) following [24]. It consists of two classes \mathcal{C}_1 and \mathcal{C}_2 of nodes of equal size, in total with N nodes. For any two nodes in the graph, if they are from the same class, they are connected by an edge independently with probability p , or if they are from different classes, the probability is q . For each node $v \in \mathcal{C}_i, i \in \{1, -1\}$, the initial feature X_v is sampled independently from a Gaussian distribution $\mathcal{N}(\mu_i, \sigma^2)$, where $\mu_i = \mathcal{C}_i, \sigma = I$. In this paper, we assign $N = 100$ and the feature dimension is 8.

I.2 Experiments Setup

For the SGC backbone, we follow the [44] setting where we run 10 runs for the fixed seed 42 and calculate the mean and the standard deviation. Furthermore, we fix the learning rate and weight decay in the same dataset and run 100 epochs for every dataset. For the GCN backbone, we follow the [16] settings where we run 5 runs from the seed $\{0, 1, 2, 3, 4\}$ and calculate the mean and the standard deviation. We fix the hidden dimension to 32 and dropout rate to 0.6. Furthermore, we fix the learning rate to be 0.005 and weight decay to be $5e-4$ and run 200 epochs for every dataset. We use the default splits in `torch_geometric`. We use Tesla-V100-SXM2-32GB in all experiments.

I.3 Time Complexity Analysis and the Modified SBP

Label-SBP As shown in equation 4.2, we maintain the positive adjacency matrix $A^+ = \hat{A}$ and construct the negative adjacency matrix A_l by assigning 1 when nodes i, j have different labels, -1 when they share the same label, and 0 when either label is unknown. We then apply softmax to A_l to normalize the negative adjacency matrix. The overall signed adjacency matrix is $A_{sign} = \alpha A^+ - \beta \text{softmax}(A_l)$, where α and β are hyperparameters. Given n_t training nodes and d edges in the graph, our Label-SBP increases the edge count from $O(d)$ to $O(n_t^2)$, thereby increasing the computational complexity to $O(n_t^2 d)$.

Feature-SBP When labels are unavailable, we propose Feature-SBP, which uses the similarity matrix of node features to create the negative adjacency matrix. As depicted in equation 4.2, we design the negative adjacency matrix as $A_f = -X_0 X_0^T$. We then apply softmax to A_f to normalize it. The overall matrix follows the same format as Label-SBP: $A_{sign} = \alpha A^+ - \beta \text{softmax}(A_f)$, where α and β are hyperparameters. The additional computational complexity primarily stems from the negative graph propagation, which involves $X_0 X_0^T \in \mathbb{R}^{n \times n}$, increasing the overall complexity to $O(n^2 d)$.

We show the computation time of different methods in the Table 8. On average, we improve performance on 8 out of 9 datasets (as shown in Table 2) with less than 0.05s overhead—even faster than three other baselines. We believe this time overhead is acceptable given the benefits it provides.

Table 8: Estimated training time of SBP on Cora dataset. All experiments are run under 2 layers. s is the abbreviation for second. Precompute time is the aggregation time across layers, train time is the update time of the SGC weight W , total time is the sum of them.

	Label-SBP	Feature-SBP	BatchNorm	ContraNorm	Residual	JKNET	DAGNN	SGC
Precompute time	0.1809s	0.1520s	0.1860s	0.1888s	0.0604s	0.0577s	0.1438s	0.1307s
Train time	0.1071s	0.1060s	0.1076s	0.1038s	0.1368s	0.1446s	0.1348s	0.1034s
Total time	0.2879s	0.2580s	0.2935s	0.2926s	0.1972s	0.2023s	0.2786s	0.2341s
Rank	6	4	8	7	1	2	5	3

Scalability of SBP on large-scale graph For large-scale graphs, we introduce a modified version Label-SBP-v2 by only removing edges when pairs of nodes belong to different classes. This approach allows Label-SBP-v2 to eliminate the computational overhead of the negative graph, further enhancing the sparsity of large-scale graphs. For Feature-SBP, as the number of nodes n increases, the complexity of this matrix operation grows quadratically, i.e., $\mathcal{O}(n^2 d)$. To address this, we reorder the matrix multiplication from $-X_0 X_0^T \in \mathbb{R}^{n \times n}$ to $-X_0^T X_0 \in \mathbb{R}^{d \times d}$. This preserves the distinctiveness of node representations across the feature dimension, rather than across the node dimension as in the original node-level repulsion. The modified version of Feature-SBP can be expressed as:

$$(\text{Feature-SBP-v2}) \quad X^k = (1 - \lambda)X^{(k-1)} + \lambda(\alpha \hat{A} X^{(K)} - \beta X^{(K)} \text{softmax}(-X_0^T X_0)) \quad (49)$$

This transposed alternative has a linear complexity in the number of samples, i.e., $\mathcal{O}(nd^2)$, significantly reducing the computational burden in cases where $n \gg d$.

We compare the compute time SBP with other baselines on ogbn-arxiv dataset over 100 epochs for a fair comparison. Among all the training times of the baselines, our Label-SBP-v2 achieves the 3rd fastest time while Feature-SBP-v2 ranks 5th. Therefore, we recommend using Label-SBP-v2 for large-scale graphs since they typically have a sufficient number of node labels. We believe that although there is a slight time increase, it is acceptable given the benefits.

Table 9: Estimated training time of SBP on ogbn-arxiv dataset. All experiments are run under 2 layers and 100 epochs. s is the abbreviation for second.

	Label-SBP	Feature-SBP	BatchNorm	ContraNorm	DropEdge	SGC
Train time (s)	5.5850	6.1333	5.3872	5.8375	9.5727	5.3097
Rank	3	5	2	4	6	1

The code for the experiments will be available when our paper is acceptable. We will replace this anonymous link with a non-anonymous GitHub link after the acceptance. We implement all experiments in Python 3.9 with PyTorch Geometric on one NVIDIA Tesla V100 GPU.

I.4 Results Analysis

I.4.1 CSBM results

The comparative results of Label-SBP and Feature-SBP against SGC are presented in Table 10. As the number of layers increases, SGC’s node features suffer from oversmoothing, causing the two classes to converge and accuracy to drop by nearly 30 points from its peak at 2 layers, down to 45%. Conversely, after 300 layers, SBP maintains strong performance, with node features of different classes repelling each other. This effect limits oversmoothing to within-class interactions, and improves performance from 85 to 91 in Label-SBP and from 48 to 82 in Feature-SBP, further substantiating our approach to mitigating oversmoothing.

We visualize the node features learned by Label-SBP in Figure 9. We can see that from layer 0 to layer 200, the node features from different labels repel each other and aggregate the node features from the same labels. And we also visualize the adjacency matrix of Label-SBP and Feature-SBP in Figure 10 and Figure 11 respectively, further verifying the effectiveness of our theorem and insights.

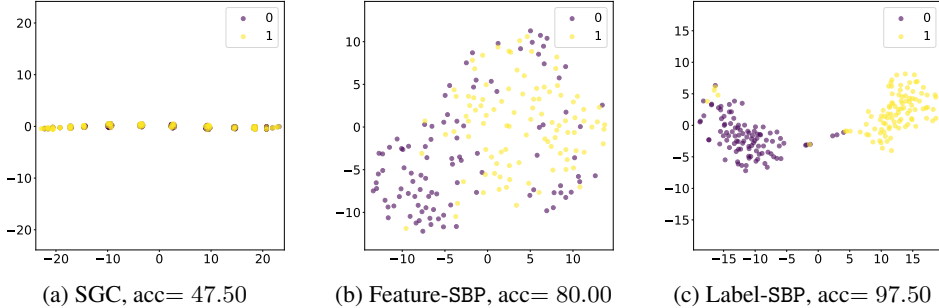


Figure 8: The t-SNE visualization of the node features and the classification accuracy from 2-CSBM and Layer= 300. Left is the result of the vallina SGC, and the middle and right are the results of SBP.

Table 10: CSBM test accuracy (%) comparison results. The best results are marked in blue on each layer. The second best results are marked in gray on each layer. We run 10 runs for the seed from 0 – 9 and demonstrate the mean \pm std in the table.

Model	#L=2	#L=5	#L=10	#L=20	#L=50	#L=100	#L=200
SGC	73.25 ± 6.90	44.50 ± 9.34	45.75 ± 9.36				
Feature-SBP	48.75 ± 5.62	53.75 ± 6.45	63.75 ± 6.25	77.00 ± 5.45	82.00 ± 4.58	82.50 ± 5.12	82.00 ± 5.45
Label-SBP	85.75 ± 4.04	93.50 ± 4.06	93.50 ± 3.57	93.50 ± 3.57	92.25 ± 3.44	93.25 ± 3.72	91.25 ± 6.05

I.4.2 GCN Results

The results for GCN are detailed in Table 11, respectively. Overall, SBP consistently outperforms all previous methods, especially in deeper layers. Beyond 16 layers in GCN, SBP maintains superior performance, affirming the effectiveness of our approach. Notably, SBP exceeds the best results of prior methods by at least 10% and up to 30% points in GCN’s deepest layers, marking significant improvements. Moreover, unlike previous methods that perform best in shallow layers, SBP excels in

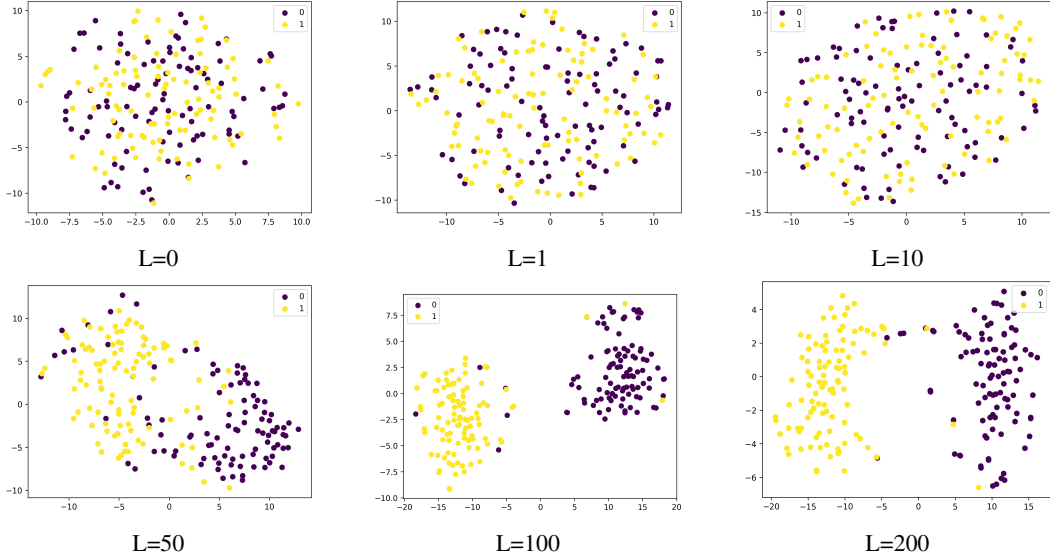


Figure 9: CSBM node features visualization. We update the features by Label-SBP. L is the propagation layer number. 0,1 represent different classes.

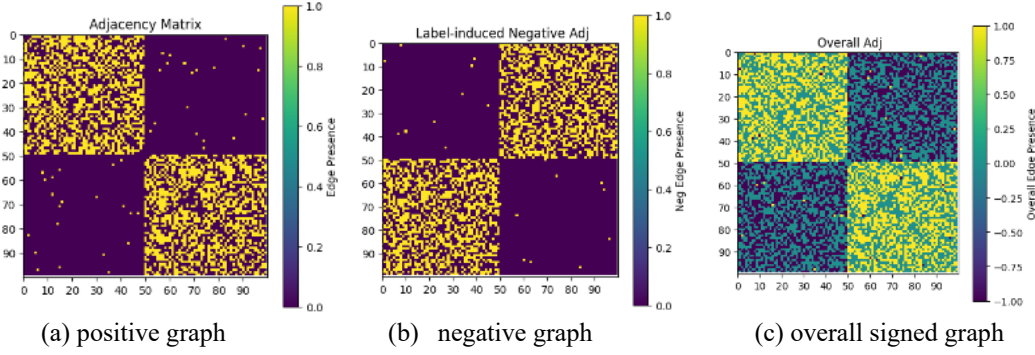


Figure 10: The visualization of the adjacency matrix of Label-SBP. Here left is the positive graph; middle is the negative graph; right is the overall signed graph.

moderately deep layers, as observed in GCN across all datasets. This further confirms the effectiveness of SBP.

I.4.3 β Analysis on Heterophilic Datasets

Our method SBP can outperform other baselines under $\beta = 1$ across different layers, so we do not tune our hyper-parameters carefully. However, since β is the weight of the negative adjacency matrix (equation 4.2) representing the repulsion between different nodes, as seen in Figure 4 and 5, the best performance of SBP appears when β is larger in the heterophilic graphs, so the result in Figure 3a(a) is not the best performance of our SBP. To further show the effectiveness of our SBP, we conduct experiments on Cornell with different β in Table 12, the best β is 20 where the performance increases 25 points in deep layer 50.

I.4.4 SBP on more benchmarks

We further compare our SBP with SGC on six additional datasets [36] in Table 13. Our SBP outperforms SGC on five out of these six datasets. We believe that these six datasets, combined with

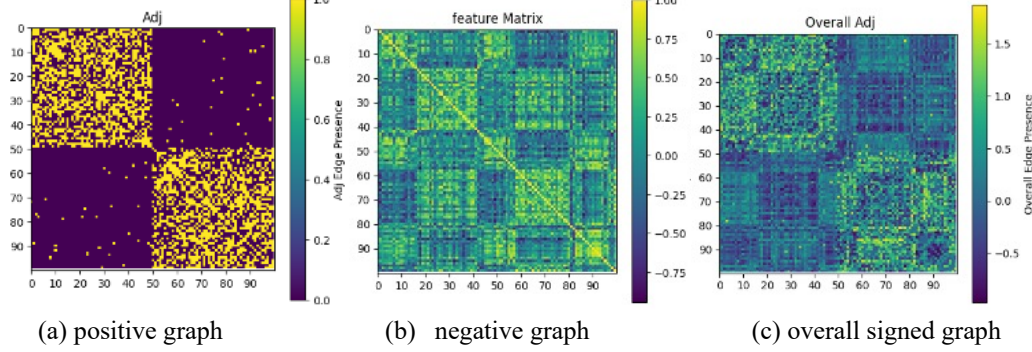


Figure 11: The visualization of the adjacency matrix of Feature-SBP. Here left is the positive graph; middle is the negative graph; right is the overall signed graph.

the nine datasets presented in Table 13 of our paper, provide sufficient evidence to demonstrate the effectiveness of our approach.

I.4.5 Different Backbones

In this paper, we focus on introducing a novel theoretic signed graph perspective for oversmoothing analysis, so we do not take many tricks into account or carefully fine-tune our hyperparameters. Thus, our results in the paper are not as comparable to previous baselines [20, 47, 48]. However, existing oversmoothing researches are indeed hard to compare, because they are often composed of multiple techniques — such as residual, BatchNorm, data augmentation — and the parameters are often heavily (over-)tuned on small-scale datasets. And it becomes clear that to attain SOTA performance, one needs to essentially compose multiple such techniques without fully understanding their individual roles. For example, GCNII uses both initial residual connection and identity map, further combined with dropout.

Our goal is to provide a new unified understanding of these techniques, so we justified it by showing that SBP as a single simple technique can attain good performance. And we believe that it would work complementarily with other techniques in the field, because oversmoothing is still challenging to solve with a very larger depth.

To further verify the effectiveness, we combine our SBP to one of the SOTA settings GCNII [20] and the results are as seen in Table 14. The results indicate that after combining our method, GCNII demonstrates greater robustness as the layers go deeper, particularly in the middle layers (layer=8), highlighting the efficacy of our signed graph insight.

I.4.6 SBP on Large-scale graphs

We conducted experiments with a larger graph ogbn-products than ogbn-arxiv under 100 epochs and 2 layers in Table 15. The results indicate that our SBP outperforms the initial GCN baselines. Given the results presented for ogbn-arxiv in Table 5 of our paper, we believe these findings adequately demonstrate the performance of our SBP on large-scale graphs.

I.4.7 Further Optimization

Based on the experiment results, we want to propose 2 strategies for further optimization.

1) hyper-parameter tuning on the negative weight β . As seen in Figures 4 and 5, we found that β influences the performance a lot, our default $\beta = 1$ for Table 2 and 3 is certainly not optimal for the above 4 homophilic datasets. We suggest tuning higher β for the heterophilic graphs since they need more repulsion and smaller for the homophilic datasets. As the layer deepens, maybe greater weight should be placed on the negative adjacency graphs to alleviate oversmoothing.

2) adapt our SBP to more effective GNNs. Our method is simple, architecture-free, without additional learnable parameters, and thus can be flexibly applied in various architectures. As seen in

Table 11: GCN test accuracy (%) comparison results. The best results are marked in blue and the second best results are marked in gray on every layer. We run 5 runs for the seed from 0 – 4 and demonstrate the mean \pm std in the table.

Model	#L=2	#L=4	#L=8	#L=16	#L=32	#L=64
<i>Cora</i> [37]						
GCN [8]	80.68 \pm 0.09	79.69 \pm 0.00	74.32 \pm 0.00	30.95 \pm 0.00	30.95 \pm 0.00	24.85 \pm 7.46
GAT [10]	81.48 \pm 0.48	80.69 \pm 0.93	58.59 \pm 1.95	25.17 \pm 5.67	31.93 \pm 0.21	28.38 \pm 0.00
wGCN [46]	80.97 \pm 0.28	80.51 \pm 0.00	80.46 \pm 1.77	70.53 \pm 22.09	80.02 \pm 0.12	27.90 \pm 6.09
BatchNorm [41]	78.09 \pm 0.00	77.87 \pm 0.02	73.62 \pm 0.57	70.79 \pm 0.00	53.90 \pm 2.19	35.32 \pm 3.41
PairNorm [17]	79.01 \pm 0.00	78.26 \pm 0.50	73.21 \pm 0.00	62.96 \pm 0.00	48.13 \pm 0.91	44.01 \pm 3.46
ContraNorm [16]	81.55 \pm 0.21	79.61 \pm 0.75	77.71 \pm 0.00	63.35 \pm 0.00	44.56 \pm 4.83	38.97 \pm 0.00
DropEdge [22]	78.38 \pm 0.00	74.47 \pm 0.00	26.91 \pm 0.83	22.24 \pm 3.04	27.18 \pm 0.00	25.98 \pm 6.00
Residual	80.68 \pm 0.09	78.77 \pm 0.00	79.26 \pm 0.21	40.91 \pm 0.00	30.95 \pm 0.00	27.90 \pm 6.09
Feature-SBP	80.44 \pm 0.83	79.26 \pm 1.18	78.56 \pm 0.59	77.22 \pm 0.55	73.65 \pm 0.48	61.62 \pm 5.24
Label-SBP	80.31 \pm 0.70	79.16 \pm 1.30	79.50 \pm 0.00	77.43 \pm 1.49	74.52 \pm 0.36	65.02 \pm 2.97
<i>CiteSeer</i> [38]						
GCN [8]	67.45 \pm 0.54	65.62 \pm 0.25	37.22 \pm 2.46	22.03 \pm 4.76	19.65 \pm 0.00	19.65 \pm 0.00
GAT [10]	69.91 \pm 0.86	67.47 \pm 0.22	44.71 \pm 3.07	23.48 \pm 1.36	24.40 \pm 0.40	25.95 \pm 2.17
wGCN [46]	66.21 \pm 0.63	66.49 \pm 0.69	66.79 \pm 0.00	57.54 \pm 18.94	19.65 \pm 0.00	19.65 \pm 0.00
BatchNorm [41]	63.44 \pm 0.94	62.34 \pm 0.25	61.36 \pm 0.00	50.58 \pm 1.24	41.41 \pm 0.00	35.00 \pm 1.09
PairNorm [17]	63.58 \pm 0.63	64.32 \pm 0.95	61.95 \pm 1.24	50.06 \pm 0.00	37.21 \pm 1.87	36.09 \pm 0.07
ContraNorm [16]	66.83 \pm 0.49	64.78 \pm 0.92	60.70 \pm 0.60	44.79 \pm 1.65	37.36 \pm 0.25	30.85 \pm 0.81
DropEdge [22]	63.86 \pm 0.03	62.24 \pm 0.90	24.73 \pm 5.72	20.65 \pm 0.00	20.04 \pm 0.19	19.95 \pm 0.09
Residual	67.45 \pm 0.54	66.21 \pm 0.16	67.34 \pm 0.00	33.21 \pm 0.00	19.65 \pm 0.00	19.65 \pm 0.00
Feature-SBP	67.38 \pm 0.66	66.94 \pm 0.00	66.29 \pm 0.02	65.35 \pm 1.99	61.43 \pm 0.00	42.09 \pm 1.65
Label-SBP	67.23 \pm 0.64	66.72 \pm 0.00	66.29 \pm 0.89	65.50 \pm 2.13	59.93 \pm 0.85	44.41 \pm 1.57
<i>PubMed</i> [39]						
GCN [8]	76.44 \pm 0.34	76.52 \pm 0.32	69.58 \pm 5.89	39.92 \pm 0.00	39.92 \pm 0.00	39.92 \pm 0.00
+BatchNorm [41]	75.52 \pm 0.12	77.15 \pm 0.00	77.10 \pm 0.00	76.92 \pm 0.00	75.43 \pm 0.00	69.33 \pm 1.01
+PairNorm [17]	75.66 \pm 0.11	76.71 \pm 0.00	77.99 \pm 0.00	77.22 \pm 0.39	75.52 \pm 2.02	71.22 \pm 3.68
+ContraNorm [16]	76.05 \pm 0.33	78.42 \pm 0.00	OOM	OOM	OOM	OOM
+DropEdge [22]	73.41 \pm 0.03	73.96 \pm 0.79	52.51 \pm 10.91	40.27 \pm 0.00	39.90 \pm 0.59	40.08 \pm 0.39
+Residual	76.44 \pm 0.34	77.28 \pm 0.00	77.38 \pm 0.00	63.14 \pm 3.05	39.92 \pm 0.00	39.92 \pm 0.00
Feature-SBP	75.72 \pm 0.06	76.84 \pm 0.00	78.39 \pm 0.00	79.71 \pm 0.00	77.59 \pm 0.23	78.06 \pm 0.13
Label-SBP	76.33 \pm 0.25	76.91 \pm 0.00	77.60 \pm 0.49	76.31 \pm 0.00	77.17 \pm 0.67	78.01 \pm 0.16

Table 12: Ablation study of negative weight β on Cornell dataset.

Layer	2	5	10	20	50
$\beta = 0.1$	72.97 \pm 0.00	67.57 \pm 0.00	51.53 \pm 0.00	35.14 \pm 0.00	29.73 \pm 0.00
$\beta = 1$ (default)	72.97 \pm 0.00	67.57 \pm 0.00	51.53 \pm 0.00	45.95 \pm 0.00	35.14 \pm 0.00
$\beta = 10$	70.27 \pm 0.00	67.57 \pm 0.00	58.11 \pm 1.35	51.53 \pm 0.00	51.53 \pm 0.00
$\beta = 20$ (best)	70.27 \pm 0.00	70.27 \pm 0.00	67.57 \pm 0.00	59.46 \pm 0.00	59.46 \pm 0.00
$\beta = 50$	64.60 \pm 0.00	40.54 \pm 0.00	40.54 \pm 0.00	40.54 \pm 0.00	40.54 \pm 0.00

Appendix I.4.5, we adapt our SBP to the GCNII models, and the results increase more than adaptation in vanilla GNN as shown in Table 2 and 3. Besides, compared to the GCNII, our SBP is more robust and stable to the layers as seen in Table 14.

Table 13: Performance Comparison on more datasets

	actor	penny94	roman-empire	Tolokers	Questions	Minesweeper
SGC	29.18 \pm 0.10	72.56 \pm 0.05	40.83 \pm 0.03	78.18 \pm 0.02	97.09 \pm 0.00	80.43 \pm 0.00
Feature-SBP	34.93 \pm 0.02	75.68 \pm 0.01	66.48 \pm 0.02	78.24 \pm 0.04	97.14 \pm 0.02	80.00 \pm 0.00
Label-SBP	34.94 \pm 0.00	75.74 \pm 0.01	66.32 \pm 0.01	78.46 \pm 0.08	97.15 \pm 0.02	80.00 \pm 0.00

Table 14: Performance Comparison between SBP and GCNII under the GCNII settings on Cora and Citessers datasets

		2	4	8	16	32	64
Cora	GCNII	78.58 \pm 0.00	77.76 \pm 0.24	73.47 \pm 3.82	78.12 \pm 1.32	82.54 \pm 0.00	81.34 \pm 0.53
	Label-SBP	78.74 \pm 1.54	78.87 \pm 0.00	79.14 \pm 0.35	79.17 \pm 0.41	80.86 \pm 0.32	81.38 \pm 0.30
	Feature-SBP	77.95 \pm 0.91	78.82 \pm 0.00	78.11 \pm 1.62	78.82 \pm 0.29	81.82 \pm 0.47	81.65 \pm 0.40
Citessers	GCNII	61.66 \pm 0.67	63.23 \pm 2.31	64.58 \pm 2.66	66.21 \pm 0.64	69.38 \pm 0.83	69.73 \pm 0.26
	Label-SBP	65.31 \pm 0.63	63.93 \pm 3.66	68.33 \pm 0.99	66.46 \pm 0.00	70.00 \pm 0.81	69.47 \pm 0.25
	Feature-SBP	65.63 \pm 0.87	64.43 \pm 3.55	68.44 \pm 1.19	66.94 \pm 0.00	69.98 \pm 0.93	69.66 \pm 0.28

Table 15: Performance of different models on ogbn-products dataset. Time means the runtime, the format is (hour: minutes: seconds).

Method	Accuracy	Time
GCN	73.96	00:06:33
BatchNorm	74.93	00:06:18
Feature-SBP	74.90	00:06:43
Label-SBP	76.62	00:06:39

NeurIPS Paper Checklist

1. Claims

Question: Do the main claims made in the abstract and introduction accurately reflect the paper’s contributions and scope?

Answer: **[Yes]**

Justification: The main claims made in the abstract and introduction accurately reflect the paper’s contributions and scope.

Guidelines:

- The answer NA means that the abstract and introduction do not include the claims made in the paper.
- The abstract and/or introduction should clearly state the claims made, including the contributions made in the paper and important assumptions and limitations. A No or NA answer to this question will not be perceived well by the reviewers.
- The claims made should match theoretical and experimental results, and reflect how much the results can be expected to generalize to other settings.
- It is fine to include aspirational goals as motivation as long as it is clear that these goals are not attained by the paper.

2. Limitations

Question: Does the paper discuss the limitations of the work performed by the authors?

Answer: **[Yes]**

Justification: We discuss the limitations.

Guidelines:

- The answer NA means that the paper has no limitation while the answer No means that the paper has limitations, but those are not discussed in the paper.
- The authors are encouraged to create a separate "Limitations" section in their paper.
- The paper should point out any strong assumptions and how robust the results are to violations of these assumptions (e.g., independence assumptions, noiseless settings, model well-specification, asymptotic approximations only holding locally). The authors should reflect on how these assumptions might be violated in practice and what the implications would be.
- The authors should reflect on the scope of the claims made, e.g., if the approach was only tested on a few datasets or with a few runs. In general, empirical results often depend on implicit assumptions, which should be articulated.

- The authors should reflect on the factors that influence the performance of the approach. For example, a facial recognition algorithm may perform poorly when image resolution is low or images are taken in low lighting. Or a speech-to-text system might not be used reliably to provide closed captions for online lectures because it fails to handle technical jargon.
- The authors should discuss the computational efficiency of the proposed algorithms and how they scale with dataset size.
- If applicable, the authors should discuss possible limitations of their approach to address problems of privacy and fairness.
- While the authors might fear that complete honesty about limitations might be used by reviewers as grounds for rejection, a worse outcome might be that reviewers discover limitations that aren't acknowledged in the paper. The authors should use their best judgment and recognize that individual actions in favor of transparency play an important role in developing norms that preserve the integrity of the community. Reviewers will be specifically instructed to not penalize honesty concerning limitations.

3. Theory assumptions and proofs

Question: For each theoretical result, does the paper provide the full set of assumptions and a complete (and correct) proof?

Answer: **[Yes]**

Justification: Refer to Section 4 and Appendix C and D.

Guidelines:

- The answer NA means that the paper does not include theoretical results.
- All the theorems, formulas, and proofs in the paper should be numbered and cross-referenced.
- All assumptions should be clearly stated or referenced in the statement of any theorems.
- The proofs can either appear in the main paper or the supplemental material, but if they appear in the supplemental material, the authors are encouraged to provide a short proof sketch to provide intuition.
- Inversely, any informal proof provided in the core of the paper should be complemented by formal proofs provided in appendix or supplemental material.
- Theorems and Lemmas that the proof relies upon should be properly referenced.

4. Experimental result reproducibility

Question: Does the paper fully disclose all the information needed to reproduce the main experimental results of the paper to the extent that it affects the main claims and/or conclusions of the paper (regardless of whether the code and data are provided or not)?

Answer: **[Yes]**

Justification: Refer to Section 5 for implementation. We will release the code and models when this paper is published.

Guidelines:

- The answer NA means that the paper does not include experiments.
- If the paper includes experiments, a No answer to this question will not be perceived well by the reviewers: Making the paper reproducible is important, regardless of whether the code and data are provided or not.
- If the contribution is a dataset and/or model, the authors should describe the steps taken to make their results reproducible or verifiable.
- Depending on the contribution, reproducibility can be accomplished in various ways. For example, if the contribution is a novel architecture, describing the architecture fully might suffice, or if the contribution is a specific model and empirical evaluation, it may be necessary to either make it possible for others to replicate the model with the same dataset, or provide access to the model. In general, releasing code and data is often one good way to accomplish this, but reproducibility can also be provided via detailed instructions for how to replicate the results, access to a hosted model (e.g., in the case of a large language model), releasing of a model checkpoint, or other means that are appropriate to the research performed.

- While NeurIPS does not require releasing code, the conference does require all submissions to provide some reasonable avenue for reproducibility, which may depend on the nature of the contribution. For example
 - (a) If the contribution is primarily a new algorithm, the paper should make it clear how to reproduce that algorithm.
 - (b) If the contribution is primarily a new model architecture, the paper should describe the architecture clearly and fully.
 - (c) If the contribution is a new model (e.g., a large language model), then there should either be a way to access this model for reproducing the results or a way to reproduce the model (e.g., with an open-source dataset or instructions for how to construct the dataset).
 - (d) We recognize that reproducibility may be tricky in some cases, in which case authors are welcome to describe the particular way they provide for reproducibility. In the case of closed-source models, it may be that access to the model is limited in some way (e.g., to registered users), but it should be possible for other researchers to have some path to reproducing or verifying the results.

5. Open access to data and code

Question: Does the paper provide open access to the data and code, with sufficient instructions to faithfully reproduce the main experimental results, as described in supplemental material?

Answer: [\[Yes\]](#)

Justification: We provide the code in the supplemental material.

Guidelines:

- The answer NA means that paper does not include experiments requiring code.
- Please see the NeurIPS code and data submission guidelines (<https://nips.cc/public/guides/CodeSubmissionPolicy>) for more details.
- While we encourage the release of code and data, we understand that this might not be possible, so “No” is an acceptable answer. Papers cannot be rejected simply for not including code, unless this is central to the contribution (e.g., for a new open-source benchmark).
- The instructions should contain the exact command and environment needed to run to reproduce the results. See the NeurIPS code and data submission guidelines (<https://nips.cc/public/guides/CodeSubmissionPolicy>) for more details.
- The authors should provide instructions on data access and preparation, including how to access the raw data, preprocessed data, intermediate data, and generated data, etc.
- The authors should provide scripts to reproduce all experimental results for the new proposed method and baselines. If only a subset of experiments are reproducible, they should state which ones are omitted from the script and why.
- At submission time, to preserve anonymity, the authors should release anonymized versions (if applicable).
- Providing as much information as possible in supplemental material (appended to the paper) is recommended, but including URLs to data and code is permitted.

6. Experimental setting/details

Question: Does the paper specify all the training and test details (e.g., data splits, hyperparameters, how they were chosen, type of optimizer, etc.) necessary to understand the results?

Answer: [\[Yes\]](#)

Justification: Refer to Section 5.

Guidelines:

- The answer NA means that the paper does not include experiments.
- The experimental setting should be presented in the core of the paper to a level of detail that is necessary to appreciate the results and make sense of them.

- The full details can be provided either with the code, in appendix, or as supplemental material.

7. Experiment statistical significance

Question: Does the paper report error bars suitably and correctly defined or other appropriate information about the statistical significance of the experiments?

Answer: [Yes]

Justification: We experiments on five random seeds and provide the mean and std in Table ??.

Guidelines:

- The answer NA means that the paper does not include experiments.
- The authors should answer "Yes" if the results are accompanied by error bars, confidence intervals, or statistical significance tests, at least for the experiments that support the main claims of the paper.
- The factors of variability that the error bars are capturing should be clearly stated (for example, train/test split, initialization, random drawing of some parameter, or overall run with given experimental conditions).
- The method for calculating the error bars should be explained (closed form formula, call to a library function, bootstrap, etc.)
- The assumptions made should be given (e.g., Normally distributed errors).
- It should be clear whether the error bar is the standard deviation or the standard error of the mean.
- It is OK to report 1-sigma error bars, but one should state it. The authors should preferably report a 2-sigma error bar than state that they have a 96% CI, if the hypothesis of Normality of errors is not verified.
- For asymmetric distributions, the authors should be careful not to show in tables or figures symmetric error bars that would yield results that are out of range (e.g. negative error rates).
- If error bars are reported in tables or plots, The authors should explain in the text how they were calculated and reference the corresponding figures or tables in the text.

8. Experiments compute resources

Question: For each experiment, does the paper provide sufficient information on the computer resources (type of compute workers, memory, time of execution) needed to reproduce the experiments?

Answer: [Yes]

Justification: Refer to Section 5.3.

Guidelines:

- The answer NA means that the paper does not include experiments.
- The paper should indicate the type of compute workers CPU or GPU, internal cluster, or cloud provider, including relevant memory and storage.
- The paper should provide the amount of compute required for each of the individual experimental runs as well as estimate the total compute.
- The paper should disclose whether the full research project required more compute than the experiments reported in the paper (e.g., preliminary or failed experiments that didn't make it into the paper).

9. Code of ethics

Question: Does the research conducted in the paper conform, in every respect, with the NeurIPS Code of Ethics <https://neurips.cc/public/EthicsGuidelines>?

Answer: [Yes]

Justification: The research conforms with the NeurIPS Code of Ethics.

Guidelines:

- The answer NA means that the authors have not reviewed the NeurIPS Code of Ethics.

- If the authors answer No, they should explain the special circumstances that require a deviation from the Code of Ethics.
- The authors should make sure to preserve anonymity (e.g., if there is a special consideration due to laws or regulations in their jurisdiction).

10. Broader impacts

Question: Does the paper discuss both potential positive societal impacts and negative societal impacts of the work performed?

Answer: **[No]**

Justification: There is no societal impact of the work performed.

Guidelines:

- The answer NA means that there is no societal impact of the work performed.
- If the authors answer NA or No, they should explain why their work has no societal impact or why the paper does not address societal impact.
- Examples of negative societal impacts include potential malicious or unintended uses (e.g., disinformation, generating fake profiles, surveillance), fairness considerations (e.g., deployment of technologies that could make decisions that unfairly impact specific groups), privacy considerations, and security considerations.
- The conference expects that many papers will be foundational research and not tied to particular applications, let alone deployments. However, if there is a direct path to any negative applications, the authors should point it out. For example, it is legitimate to point out that an improvement in the quality of generative models could be used to generate deepfakes for disinformation. On the other hand, it is not needed to point out that a generic algorithm for optimizing neural networks could enable people to train models that generate Deepfakes faster.
- The authors should consider possible harms that could arise when the technology is being used as intended and functioning correctly, harms that could arise when the technology is being used as intended but gives incorrect results, and harms following from (intentional or unintentional) misuse of the technology.
- If there are negative societal impacts, the authors could also discuss possible mitigation strategies (e.g., gated release of models, providing defenses in addition to attacks, mechanisms for monitoring misuse, mechanisms to monitor how a system learns from feedback over time, improving the efficiency and accessibility of ML).

11. Safeguards

Question: Does the paper describe safeguards that have been put in place for responsible release of data or models that have a high risk for misuse (e.g., pretrained language models, image generators, or scraped datasets)?

Answer: **[Yes]**

Justification: This paper describes safeguards that have been put in place for the responsible release of data or models that have a high risk.

Guidelines:

- The answer NA means that the paper poses no such risks.
- Released models that have a high risk for misuse or dual-use should be released with necessary safeguards to allow for controlled use of the model, for example by requiring that users adhere to usage guidelines or restrictions to access the model or implementing safety filters.
- Datasets that have been scraped from the Internet could pose safety risks. The authors should describe how they avoided releasing unsafe images.
- We recognize that providing effective safeguards is challenging, and many papers do not require this, but we encourage authors to take this into account and make a best faith effort.

12. Licenses for existing assets

Question: Are the creators or original owners of assets (e.g., code, data, models), used in the paper, properly credited and are the license and terms of use explicitly mentioned and properly respected?

Answer: [Yes]

Justification: We cite all papers that produced the code package or dataset.

Guidelines:

- The answer NA means that the paper does not use existing assets.
- The authors should cite the original paper that produced the code package or dataset.
- The authors should state which version of the asset is used and, if possible, include a URL.
- The name of the license (e.g., CC-BY 4.0) should be included for each asset.
- For scraped data from a particular source (e.g., website), the copyright and terms of service of that source should be provided.
- If assets are released, the license, copyright information, and terms of use in the package should be provided. For popular datasets, paperswithcode.com/datasets has curated licenses for some datasets. Their licensing guide can help determine the license of a dataset.
- For existing datasets that are re-packaged, both the original license and the license of the derived asset (if it has changed) should be provided.
- If this information is not available online, the authors are encouraged to reach out to the asset's creators.

13. New assets

Question: Are new assets introduced in the paper well documented and is the documentation provided alongside the assets?

Answer: [Yes]

Justification: The new assets introduced in the paper are well documented and the documentation is provided.

Guidelines:

- The answer NA means that the paper does not release new assets.
- Researchers should communicate the details of the dataset/code/model as part of their submissions via structured templates. This includes details about training, license, limitations, etc.
- The paper should discuss whether and how consent was obtained from people whose asset is used.
- At submission time, remember to anonymize your assets (if applicable). You can either create an anonymized URL or include an anonymized zip file.

14. Crowdsourcing and research with human subjects

Question: For crowdsourcing experiments and research with human subjects, does the paper include the full text of instructions given to participants and screenshots, if applicable, as well as details about compensation (if any)?

Answer: [NA]

Justification: The paper does not involve crowdsourcing nor research with human subjects.

Guidelines:

- The answer NA means that the paper does not involve crowdsourcing nor research with human subjects.
- Including this information in the supplemental material is fine, but if the main contribution of the paper involves human subjects, then as much detail as possible should be included in the main paper.
- According to the NeurIPS Code of Ethics, workers involved in data collection, curation, or other labor should be paid at least the minimum wage in the country of the data collector.

15. Institutional review board (IRB) approvals or equivalent for research with human subjects

Question: Does the paper describe potential risks incurred by study participants, whether such risks were disclosed to the subjects, and whether Institutional Review Board (IRB) approvals (or an equivalent approval/review based on the requirements of your country or institution) were obtained?

Answer: [NA]

Justification: The paper does not involve crowdsourcing nor research with human subjects.

Guidelines:

- The answer NA means that the paper does not involve crowdsourcing nor research with human subjects.
- Depending on the country in which research is conducted, IRB approval (or equivalent) may be required for any human subjects research. If you obtained IRB approval, you should clearly state this in the paper.
- We recognize that the procedures for this may vary significantly between institutions and locations, and we expect authors to adhere to the NeurIPS Code of Ethics and the guidelines for their institution.
- For initial submissions, do not include any information that would break anonymity (if applicable), such as the institution conducting the review.

16. Declaration of LLM usage

Question: Does the paper describe the usage of LLMs if it is an important, original, or non-standard component of the core methods in this research? Note that if the LLM is used only for writing, editing, or formatting purposes and does not impact the core methodology, scientific rigorousness, or originality of the research, declaration is not required.

Answer: [NA]

Justification: The core method development in this research does not involve LLMs as any important, original, or non-standard components.

Guidelines:

- The answer NA means that the core method development in this research does not involve LLMs as any important, original, or non-standard components.
- Please refer to our LLM policy (<https://neurips.cc/Conferences/2025/LLM>) for what should or should not be described.